The Plant Cell, Vol. 19: 2140–2155, July 2007, www.plantcell.org © 2007 American Society of Plant Biologists

Molecular Interactions of a Soluble Gibberellin Receptor, GID1, with a Rice DELLA Protein, SLR1, and Gibberellin [W]

Miyako Ueguchi-Tanaka,[a,1,2] Masatoshi Nakajima,[b,1] Etsuko Katoh,[c,1] Hiroko Ohmiya,[a] Kenji Asano,[a] Shoko Saji,[c] Xiang Hongyu,[c] Motoyuki Ashikari,[a] Hidemi Kitano,[a] Isomaro Yamaguchi,[d] and Makoto Matsuoka[a]

[a] Bioscience and Biotechnology Center, Nagoya University, Nagoya 464-8601, Japan
[b] Department of Applied Biological Chemistry, University of Tokyo, Tokyo 113-8657, Japan
[c] Department of Biochemistry, National Institute of Agrobiological Sciences, Tsukuba 305-8602, Japan
[d] Department of Biotechnology, Maebashi Institute of Technology, Gunma 371-0816, Japan

***GIBBERELLIN INSENSITIVE DWARF1* (*GID1*) encodes a soluble gibberellin (GA) receptor that shares sequence similarity with a hormone-sensitive lipase (HSL). Previously, a yeast two-hybrid (Y2H) assay revealed that the GID1-GA complex directly interacts with SLENDER RICE1 (SLR1), a DELLA repressor protein in GA signaling. Here, we demonstrated, by pull-down and bimolecular fluorescence complementation (BiFC) experiments, that the GA-dependent GID1–SLR1 interaction also occurs in planta. GA_4 was found to have the highest affinity to GID1 in Y2H assays and is the most effective form of GA in planta. Domain analyses of SLR1 using Y2H, gel filtration, and BiFC methods revealed that the DELLA and TVHYNP domains of SLR1 are required for the GID1–SLR1 interaction. To identify the important regions of GID1 for GA and SLR1 interactions, we used many different mutant versions of GID1, such as the spontaneous mutant GID1s, N- and C-terminal truncated GID1s, and mutagenized GID1 proteins with conserved amino acids replaced with Ala. The amino acid residues important for SLR1 interaction completely overlapped the residues required for GA binding that were scattered throughout the GID1 molecule. When we plotted these residues on the GID1 structure predicted by analogy with HSL tertiary structure, many residues were located at regions corresponding to the substrate binding pocket and lid. Furthermore, the GA–GID1 interaction was stabilized by SLR1. Based on these observations, we proposed a molecular model for interaction between GA, GID1, and SLR1.**

INTRODUCTION

Gibberellins (GAs) are a large family of tetracyclic diterpenoid plant hormones that induce a wide range of plant growth responses, including seed germination, stem elongation, leaf expansion, induction of flowering, and pollen maturation (Davies, 1995).

One of the most important factors in GA signaling is the GA receptor. Recently, a soluble GA receptor was isolated through analysis of a rice (*Oryza sativa*) *GA insensitive dwarf1* (*gid1*) mutant (Ueguchi-Tanaka et al., 2005). The *GID1* gene encodes an unknown protein preferentially localized in the nucleus that interacts with biologically active GAs in vitro with reasonable affinity. Nakajima et al. (2006) isolated three homologous genes in *Arabidopsis thaliana* (At *GID1a*, At *GID1b*, and At *GID1c*) that encode highly similar proteins to rice GID1. In vitro GA binding experiments conducted with recombinant proteins confirmed that these *Arabidopsis* proteins function similarly to rice GID1 in terms of ligand selectivity and affinity. Recently, Griffiths et al. (2006), Willige et al. (2007), and Iuchi et al. (2007) showed that triple mutations in At *GID1a*, At *GID1b*, and At *GID1c* resulted in a severe dwarf phenotype that was GA insensitive. These observations demonstrate that the GID1 proteins function in GA signaling in *Arabidopsis* as in rice.

The overall primary structure of these GID1s is similar to that of the hormone-sensitive lipase (HSL) family (Ueguchi-Tanaka et al., 2005). HSL was first recognized as an enzyme involved in lipid metabolism, including the hydrolysis of triacylglycerol (Yeaman, 2004). Now some bacterial esterases are also classified in the HSL family, though they are not involved in lipid metabolism (Wei et al., 1999; De Simone et al., 2000, 2001). Proteins in the HSL family form the α/β hydrolase fold that is composed of a mostly parallel, eight-stranded β-sheet surrounded by α-helices (Osterlund, 2001). Since the α/β hydrolase fold is constructed of conserved motifs in the HSL family and is important for the substrate–enzyme interactions of these proteins, this fold may also mediate the interaction between GID1 and GA. However, the GID1 protein lacks a single, well-conserved amino acid residue essential for HSL activity and did not show hydrolase activity with *p*-nitrophenyl acetate, a substrate often used to detect hydrolase activity (Ueguchi-Tanaka et al., 2005).

Another important factor in GA signaling is the DELLA protein, which acts as a repressor of GA signaling (Peng et al., 1997, 1999; Silverstone et al., 1998; Ikeda et al., 2001; Chandler et al., 2002; Itoh et al., 2002). Rice has one DELLA protein, SLENDER RICE1 (SLR1), whereas *Arabidopsis* has five (Repressor of ga1-3 [RGA], GA-INSENSITIVE [GAI], RGA-LIKE1 [RGL1], RGL2, and RGL3). GA-dependent degradation of the DELLA protein is a key event in GA signaling, and an F-box protein, referred to as GA

[1] These authors contributed equally to this work.
[2] Address correspondence to mueguchi@agr.nagoya-u.ac.jp.
The author responsible for distribution of materials integral to the findings presented in this article in accordance with the policy described in the Instructions for Authors (www.plantcell.org) is: Miyako Ueguchi-Tanaka (mueguchi@nuagr1.agr.nagoya-u.ac.jp).
[W] Online version contains Web-only data.
www.plantcell.org/cgi/doi/10.1105/tpc.106.043729

INSENSITIVE2 (GID2) in rice and SLEEPY1 (SLY1) in *Arabidopsis*, is involved in its degradation as a component of the SCF E3 ubiquitin ligase (McGinnis et al., 2003; Sasaki et al., 2003).

The first evidence that the GID1 receptor is directly involved in the DELLA-mediated GA signaling system was obtained from a GA-dependent interaction between GID1 and SLR1 in a yeast two-hybrid (Y2H) assay (Ueguchi-Tanaka et al., 2005). Recently, three groups independently found GA-dependent interactions between At GID1(s) and the *Arabidopsis* DELLA proteins (Griffiths et al., 2006; Nakajima et al., 2006; Willige et al., 2007). Griffiths et al. (2006) and Willige et al. (2007) further analyzed the interacting domain(s) of the *Arabidopsis* DELLA proteins with At GID1a using Y2H assays and arrived at different conclusions. Griffiths et al. (2006) concluded that both the DELLA and VHYNP domains of RGA are necessary for interaction with At GID1a, while Willige et al. (2007) concluded that the VHYNP domain is not essential for the interaction between GAI and At GID1a.

In this study, we confirmed the GA-dependent GID1–SLR1 interaction in vivo and compared the GA selectivity and GA dose dependency estimated by the GID1–SLR1 interaction in Y2H assays with those of in planta GA actions, such as leaf sheath elongation and SLR1 degradation. These studies revealed that GA-dependent events occurring in rice plants are reflective of the characteristics of the GID1 molecule in yeast cells. Using Y2H assays and analyses of the in vitro interaction between GID1 and SLR1, we also identified amino acid residues of GID1 that are important for GA and SLR1 interaction and regions of SLR1 that are important for GID1 interaction. Based on these observations, a molecular model for GA-dependent GID1-SLR1 complex formation has been proposed.

RESULTS

The GA-Dependent Interaction between GID1 and SLR1 in Planta

In the previous study, we found that the GA-dependent GID1–SLR1 interaction occurs in yeast cells (Ueguchi-Tanaka et al., 2005). This is a good experimental system for studying the biochemical properties of GID1 binding to GA and GID1–SLR1 interaction, assuming that the interaction in yeast cells is reflective of the events in planta. Thus, in this study, we attempted to confirm that the GA-dependent interaction really occurs in planta. First, we performed an in vitro pull-down experiment using thioredoxin (Trx)·His-GID1 and glutathione *S*-transferase (GST)-SLR1 recombinant proteins produced in *Escherichia coli*. GST-SLR1 copurified with Trx·His-GID1 in the presence of GA_4 but not in the absence of GA_4 (see Supplemental Figure 1 online), demonstrating that GID1 binds to SLR1 in a GA-dependent manner in vitro.

We also confirmed the in vivo GID1–SLR1 interaction using rice callus lines that overproduce green fluorescent protein (GFP)-GID1. Two independent transgenic lines, line 1 and line 2, were treated with or without GA_4 for 5 min. The crude protein fractions contained GFP-GID1 and SLR1, and the amount of GFP-GID1 in line 1 was higher than line 2 (Figure 1A). When we precipitated GFP-GID1 with a GFP antibody, the SLR1 protein coimmunoprecipitated with GFP-GID1 only in the GA_4-treated extracts. The coprecipitated SLR1 consisted of two bands corresponding to nonphosphorylated and phosphorylated forms (Figure 1A, shown by closed and open circles, respectively), indicating that both forms of SLR1 interact with GID1 as previously reported (Itoh et al., 2005). This result supports the model that GA-dependent interaction between SLR1 and GID1 occurs in plant cells. However, this in vivo pull-down experiment contained one limitation. For this experiment, we had to exogenously add GA_4 to the extraction buffer to stabilize the GID1-SLR1 complex. On the other hand, when we added GA_4 to a mixture including GFP-GID1 and SLR1, both of which were independently produced in *E. coli*, the GFP antibody–precipitated fraction contained SLR1 (see Supplemental Figure 2 online). This result suggests that the in vitro GID1–SLR1 interaction might occur in the above in vivo pull-down experiment, even if the GID1-SLR1 complex could not be formed in planta.

Thus, we attempted to observe in situ GA-dependent interaction between GID1 and SLR1 using the bimolecular fluorescence complementation (BiFC) method (Abe et al., 2005). Cell suspensions of *Agrobacterium tumefaciens* carrying N-terminal enhanced yellow fluorescent protein (N·EYFP)-GID1 and C-terminal enhanced yellow fluorescent protein (C·EYFP)-SLR1 constructs were infiltrated into *Nicotiana benthamiana* leaf epidermal cells. The YFP signal, caused by interaction between N·EYFP-GID1 and C·EYFP-SLR1, was only detected in the leaf treated with GA_4 for 10 min (Figure 1B). We also tested the requirement of the DELLA and TVHYNP domains for interacting with GID1 in the in vivo BiFC experiment. Neither the C·EYFP-ΔDELLA·SLR1 construct nor the C·EYFP-ΔTVHYNP·SLR1 construct interacted with N·EYFP-GID1 to produce YFP signals in the presence of GA_4 (Figure 1B). Although the untreated cells should contain endogenous GA, no fluorescence signals were observed in leaves not treated with GA_4. This is probably because the endogenous active GA level was too low to promote sufficient interaction between the fluorescence-labeled GID1 and SLR1 proteins. These results clearly demonstrate that GID1 interacts with SLR1 in a GA-dependent manner in planta; therefore, the results of the Y2H assay reflected events that occur in planta.

Comparison of GA Selectivity and GA Dose Dependency Measured in Yeast and in Planta

Previously, we observed that GID1 preferentially binds to GA_4 in vitro compared with GA_3, although the physiological activity of GA_4 in leaf sheath elongation is lower than that of GA_3 (Ueguchi-Tanaka et al., 2005). The discrepancy between the in vitro GA preference of GID1 and the physiological effectiveness of GAs in planta suggests the presence of an unknown mechanism that differentiates between in vitro and in planta events. To clarify this point, we reexamined the GA preference of GID1 using Y2H assays. Figure 2 shows the effects of various GAs (10^{-5} M) on the GID1–SLR1 interaction in yeast cells (Figure 2A) and the dose dependency of second leaf sheath elongation in seedlings of a GA-deficient rice mutant, *Tan-Ginbozu,* after a one-drop treatment of various GAs (Figure 2B). The one-drop treatment of GAs on *Tan-Ginbozu* seedlings is a classic bioassay for estimation

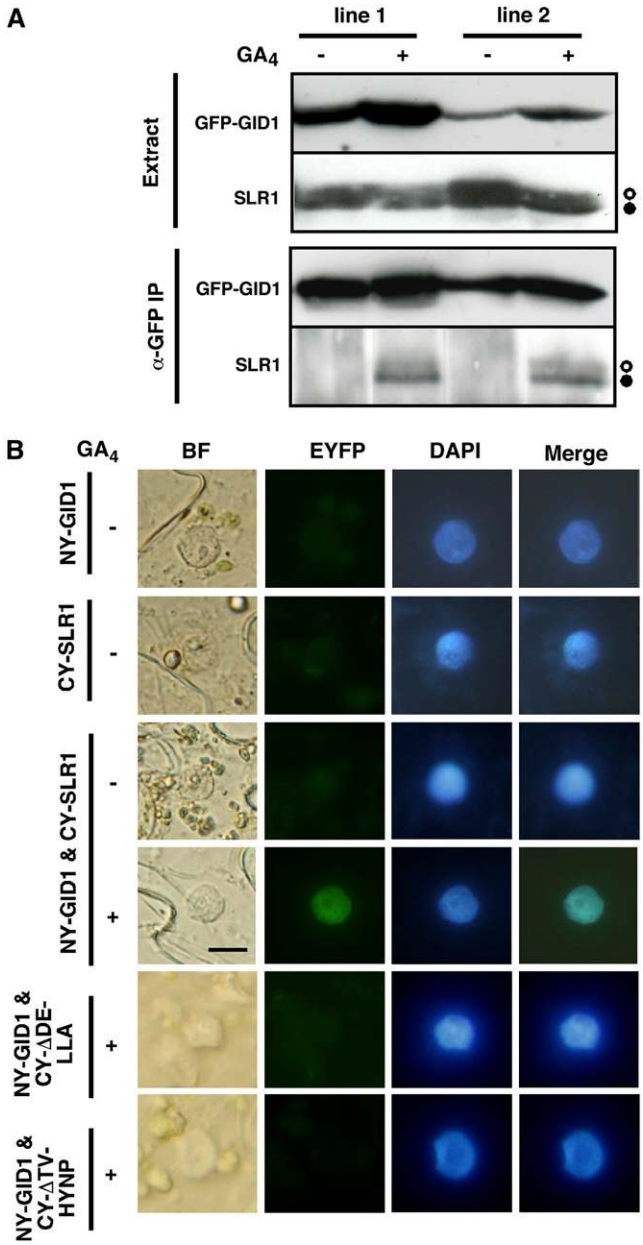

Figure 1. GA-Dependent Interaction between GID1 and SLR1 in Vivo.

(A) SLR1 was coimmunoprecipitated with GFP-GID1 in a GA-dependent manner by the GFP antibody. Each protein extract was prepared from two independent lines of transgenic rice callus overproducing GFP-GID1 (line 1 and line 2) treated with (+) or without (−) 10^{-5} M GA_4 for 5 min. Immunoblot analysis of the extract and α-GFP immunoprecipitates was performed using anti-GFP or anti-SLR1 antibody. Closed circles, nonphosphorylated SLR1; open circles, phosphorylated SLR1.

(B) BiFC analysis of in vivo interaction between GID1 and SLR1 in *N. benthamiana* leaf epidermis (Abe et al., 2005). BF, blight-field image; EYFP, EYFP fluorescence; DAPI, 4′,6-diamidino-2-phenylindole; merge, merge of EYFP and DAPI images; NY-GID1, expression of N·EYFP-GID1 alone; CY-SLR1, expression of C·EYFP-SLR1 alone; NY-GID1 and CY-SLR1, coexpression of N·EYFP-GID1 and C·EYFP-SLR1; NY-GID1 and CY-ΔDELLA, coexpression of N·EYFP-GID1 and C·EYFP-ΔDELLA·SLR1; NYGID1 and CY-ΔTVHYNP, coexpression of N·EYFP-GID1 and C·EYFP-ΔTVHYNP·SLR1. Leaves were sprayed with (+) or without (−) 10^{-4} M GA_4 10 min before observation of the signals. Bar = 10 μm.

of GA levels because *Tan-Ginbozu* seedlings sensitively and quantitatively respond to the exogenously added GA (Nishijima et al., 1993). The trend of effectiveness for various GAs in the GID1–SLR1 interaction in yeast and for leaf sheath elongation of *Tan-Ginbozu* was almost identical except for GA_3 and GA_9. For example, GA_4 and H_2-GA_4 showed the high activities in both assays, that is, GA_4 and H_2-GA_4 are the highest and the second highest in yeast, respectively, and GA_4 and H_2-GA_4 are the second and third highest for leaf sheath elongation, respectively. GA_{51} and GA_4-Me showed the lowest activities in both assays. On the other hand, GA_3 was the most effective GA for leaf sheath elongation but showed intermediate activity in the Y2H system, whereas GA_9 showed higher activity in the Y2H assay than in the leaf sheath elongation experiment.

We also examined the dose dependency of the GID1–SLR1 interaction in yeast cells with respect to GA_1, GA_3, and GA_4 (Figure 3A). GA_4 showed the highest effectiveness of the three. The interaction between GID1 and SLR1 was observed when GA_4 was present at 10^{-9} M or higher concentrations, whereas the interaction was observed at $>10^{-7}$ M of GA_1 and GA_3. The strength of the interaction increased as the GA concentration increased and reached a plateau at $\sim10^{-5}$ M for GA_4 and $\sim10^{-4}$ M for GA_1 and GA_3. The results indicate that the strength of the GID1–SLR1 interaction depends on the GA concentration. The 50% saturation point of each GA was $\sim5 \times 10^{-8}$ M for GA_4, 2×10^{-6} M for GA_3, and 3×10^{-6} M for GA_1. Then, we compared these GA dose responses of the GID1–SLR1 interaction with those for leaf sheath elongation of *Tan-Ginbozu* seedlings (Figure 3B). The 50% saturation in leaf sheath elongation was estimated to be $\sim1 \times 10^{-6}$ M for GA_4, 3×10^{-7} M for GA_3, and 4×10^{-6} M for GA_1. Thus, in the case of GA_4, the GA response of the GID1–SLR1 interaction in yeast cells was more sensitive than the response in planta. On the other hand, in the case of GA_3, the sensitivity of leaf sheath elongation was higher than that of the GID1–SLR1 interaction, whereas both sensitivities to GA_1 were almost similar, with that of yeast being a little higher. Again, the higher level of effectiveness of GA_4 than GA_3 in the GID1–SLR1 interaction in yeast cells is not consistent with lower physiological activity of GA_4 than GA_3 in *Tan-Ginbozu* seedlings.

We predicted that the higher response in leaf sheath elongation to GA_3 may be due to its stability in planta, whereas GA_4 may be rapidly inactivated in planta by GA-inactivating enzymes. To test this prediction, we examined the GA dose response for SLR1 degradation in rice seedlings and callus, which is one of the quickest events in response to GA treatment and therefore may be less disturbed by GA-inactivating enzymes. Furthermore, we observed that GA-inactivating enzymes are not expressed in rice callus (M. Ueguchi-Tanaka, unpublished results). As we expected, the most effective GA in SLR1 degradation was GA_4 in both experiments (Figures 3C and 3D). The results clearly demonstrate that GA_4 is the most effective GA among GA_1, GA_3, and GA_4 in rice cells in the absence of GA-inactivating enzymes. The reason why GA_4 is more effective than GA_3 in stimulating DELLA

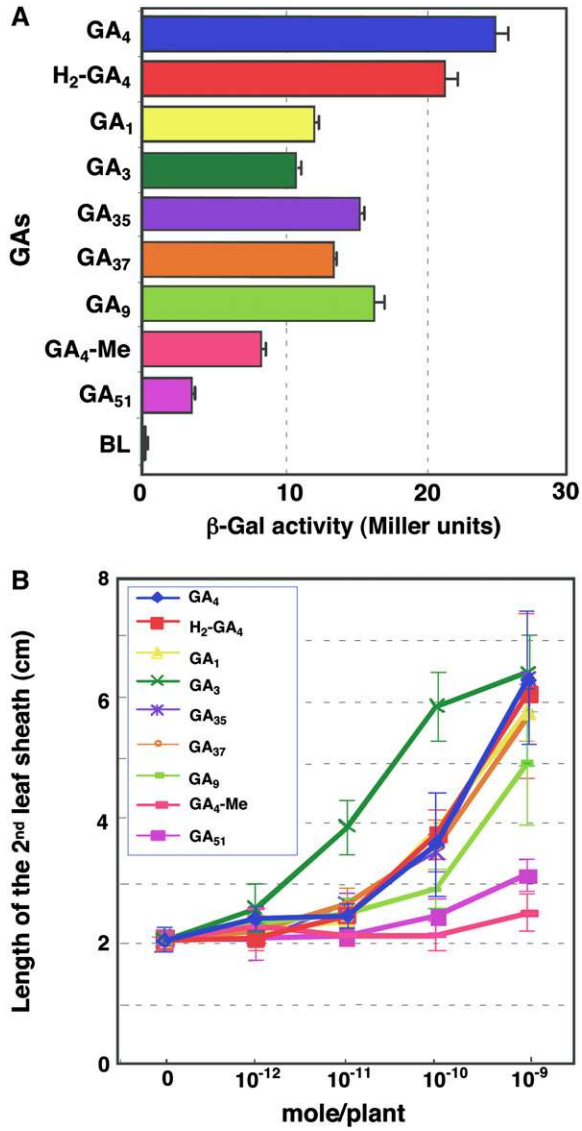

Figure 2. The Effect of Various GAs on GID1–SLR1 Interaction in Yeast Cells or on Second Leaf Sheath Elongation.

(A) Y2H assay using GID1 as bait and SLR1 as prey in the presence of 10^{-5} M various GAs. β-Gal activity was determined by a liquid assay with yeast strain Y187 transformants (means ± SD; $n = 3$). H_2-GA_4, 16,17-dihydro-GA_4; GA_4-Me, GA_4 methyl ester; BL, blank.

(B) Dose dependency of second leaf sheath elongation to various GAs in seedlings of a GA-deficient rice mutant, *Tan-Ginbozu*, by one-drop treatment (see Methods). The line colors correspond to those in **(A)**. Data are means ± SD; $n = 10$.

protein degradation, even in the leaf sheath where GA_3 is more active than GA_4, for its elongation can be explained as follows. Exogenous GA application should cause the induction of some GA-inactivating enzymes under the control of GA signaling, resulting in enhanced GA degradation activity (Sakai et al., 2003). In this context, GA_4, which can be inactivated by GA-inactivating enzymes, should be rapidly degraded in GA-treated cells; consequently, its effect should be eased. However, as GA_3 is not inactivated by inactivating enzymes, GA_3 can remain as an active form in cells even after GA treatment.

These results also indicate that the GA selectivity of GID1, as estimated by the GID1–SLR1 interaction in yeast cells, is almost the same as that in rice cells, at least with regard to the most important active GAs, GA_1, GA_3, and GA_4. However, there is one small discrepancy, that is, the relatively higher interacting activity of GA_9 in the Y2H system compared with its activity in leaf sheath elongation, which must be due to some unknown mechanism. It is possible that GA_9 might be metabolized to form the active GA in yeast.

Domain Analysis of the SLR1 Protein

To investigate the GID1 binding domain of SLR1, we analyzed SLR1 to identify essential domains for GID1 interaction in Y2H assays. First, we used a deletion series of the SLR1 cDNA as prey constructs (Figure 4A). Both plate and liquid assays showed that deletion of either the DELLA (ΔDELLA) or the TVHYNP (ΔTVHYNP) domain completely abolished the GA-dependent GID1-interacting activity of SLR1, while deletion of the space region (ΔSPACE) or the Ser/Thr-rich region (Δpoly S/T/V) did not affect its activity (Figure 4B). Deletion of the Leu zipper domain (ΔLZ) decreased the binding activity but did not diminish activity completely. Deletion of the C-terminal half of SLR1 (M1-H327), which included the most conserved regions of the GRAS family, such as the VHIID, PFYRE, and SAW domains, did not cause a complete loss of GID1 interaction; approximately one-third of the activity of the full-length SLR1 was retained. Deletion of 1.4 kb of the C-terminal region (M1-A172) led to an almost complete loss of the β-galactosidase (β-Gal) activity in the liquid assay, but the plate assay still showed that the GA-dependent interaction between the proteins occurred. Further deletion of the C-terminal side, including the TVHYNP domain (M1-E104), abolished growth on GA-containing plates. These results demonstrate that the DELLA and TVHYNP domains are essential for interaction of SLR1 with GID1, while the C-terminal side from the poly S/T/V region is not.

Furthermore, we analyzed the in vitro formation of a GA-GID1-SLR1 complex by gel filtration on Superdex-200 (Figure 5). For this analysis, we first attempted to produce the full-length recombinant SLR1 with a Trx·His tag, but we could not produce sufficient quantities of the full-length SLR1 protein. ΔSLR1s with C-terminal truncations, such as Trx·His-SLR1 (M1-H327) and Trx·His-SLR1 (M1-A172), were produced in sufficient quantities, so we used these soluble, recombinant proteins for the in vitro experiment. The internal deletions of SLR1, such as ΔDELLA, ΔSPACE, and ΔTVHYNP, were produced from Trx·His-SLR1 (M1-A172).

Trx·His-GID1 was eluted from the column in the expected fractions (~63 kD) corresponding to its molecular weight (MW) estimated by SDS-PAGE (~65 kD) and the theoretical MW (GID1 [39 kD] + Trx·His [21 kD]) (Figure 5A, A-1). On the other hand, Trx·His-SLR1 (M1-A172) was eluted at a much larger size (~85 kD) than its estimated MW on SDS-PAGE (~40 kD), which corresponded to the theoretical monomer SLR1 (M1-A172)

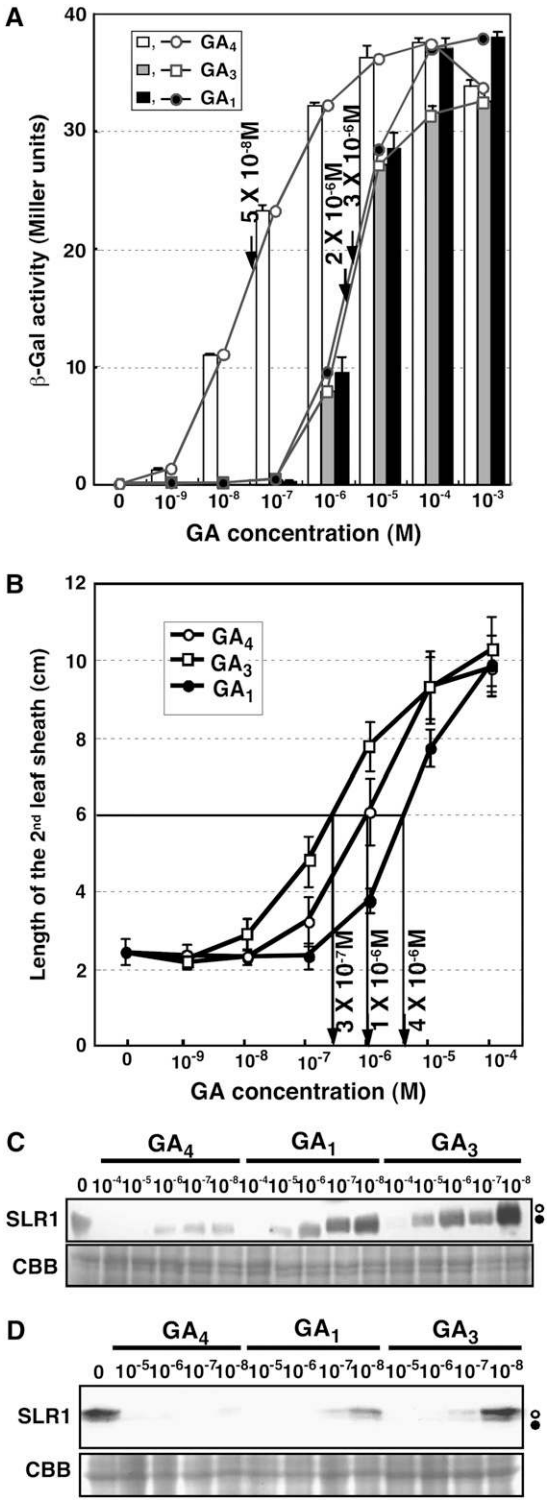

Figure 3. The Dose Dependency of GA_1, GA_3, and GA_4 for GID1–SLR1 Interaction in Y2H and for in Vivo GA Responses in Rice Cells.

(A) Y2H assay using GID1 as bait and SLR1 as prey in the presence of various concentrations of GA_1, GA_3, or GA_4. β-Gal activity was determined as in Figure 2A. Data are means ± SD, $n = 3$. The 50% saturation points are indicated by arrows.

(17 kD) + Trx·His (21 kD) (Figure 5A, A-2, top). We suspected that the Trx·His tag sequence might cause oligomerization of Trx·His-SLR1. Therefore, we analyzed the elution of Trx·His-SLR1 (M1-A172) after processing the tag. The detagged SLR1 (M1-A172) was also eluted at a larger size (~63 kD) than its estimated MW on SDS-PAGE (~20 kD), which almost corresponded to the theoretical monomer MW (17 kD) (Figure 5A, A-3), indicating that the larger size of Trx·His-SLR1 (M1-A172) in gel filtration is caused by dimer (tagged SLR1) or trimer (detagged SLR1) formation via SLR1 itself.

Then, using this gel filtration assay, we examined the in vitro interaction between Trx·His-GID1 and truncated versions of Trx·His-SLR1. When we chromatographed a mixture containing Trx·His-GID1 and Trx·His-SLR1 (M1-A172) in the absence of GA, two adjacent peaks that corresponded to those of Trx·His-SLR1 (M1-A172) (peak 1) and Trx·His-GID1 (peak 2) were observed (Figure 5A, A-2). These peaks contained the tagged GID1 and SLR1 (M1-A172) since these proteins have similar MWs. When we added GA_3 to the mixture and to the elution buffer for chromatography, the peaks corresponding to the tagged GID1 and SLR1 (M1-A172) almost disappeared and a new peak appeared at higher MW fractions (indicated by an asterisk). SDS-PAGE revealed that the fractions contained Trx·His-GID1 and Trx·His-SLR1 (M1-A172), and its estimated MW by gel filtration (~110 kD) was almost comparable to the theoretical value for a 1:1 complex of Trx·His-GID1 (63 kD) and Trx·His-SLR1 (M1-A172) (39 kD), indicating that this peak is derived from the GID1-SLR1 (M1-A172) complex in a one-to-one ratio. To exclude the possibility that the Trx·His tag influenced the interaction between GID1 and SLR1, we also performed the same experiment using detagged GID1 and SLR1 (M1-A172). The retention time of the detagged complex was almost comparable to the theoretical MW (data not shown), indicating that the Trx·His tag did not contribute to the interaction between GID1 and SLR1.

Similarly, a new peak appeared (indicated by an asterisk in Figure 5B, B-1) when Trx·His-SLR1 (M1-H327) was incubated with GID1 in the presence of GA, indicating the in vitro formation of GID1-SLR1 (M1-H327). In fact, the new peak contained the Trx·His-GID1 and Trx·His-SLR1 (M1-H327) proteins. By contrast, Trx·His-SLR1 (M1~E104), Trx·His-SLR1 (M1-A172 ΔDELLA), or Trx·His-SLR1 (M1-A172 ΔTVHYNP) did not produce any new peaks with higher MWs even under excess GA conditions (Figure 5B, B-2, B-3, and B-5). This result indicates that these deleted SLR1s cannot form GID1-SLR1 complexes in vitro. SDS-PAGE confirmed that the higher MW peak fractions of the mixtures of GID1/Trx·His-SLR1 (M1-A172 ΔDELLA) and GID1/Trx·His-SLR1 (M1-A172 ΔTVHYNP) contained only SLR1 protein, while the

(B) Second leaf sheath elongation in seedlings of a GA-deficient rice mutant, *Tan-Ginbozu*, treated with various concentrations of GA_1, GA_3, or GA_4. Data are means ± SD, $n = 10$. The 50% saturation points are indicated by arrows.

(C) and **(D)** Degradation of SLR1 protein in rice cells treated with various concentrations of GA_1, GA_3, or GA_4. The seedling of *Tan-Ginbozu* **(C)** and the wild callus **(D)** were treated with GAs for 2 h and 5 min, respectively. Immunoblot analyses were performed using anti-SLR1 antibody. Closed circles, nonphosphorylated SLR1; open circles, phosphorylated SLR1.

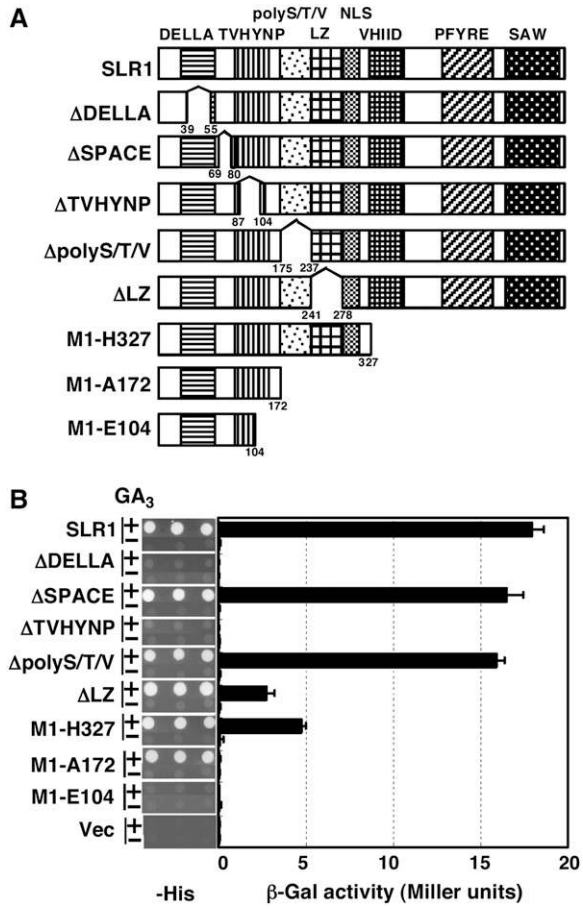

Figure 4. DELLA and TVHYNP Domains Are Essential for Interaction between GID1 and SLR1 in the Y2H Assay.

(A) Diagrams showing the SLR1 deletion constructs tested in the Y2H assay.

(B) Y2H assay using full-length GID1s as baits and the SLR1s deletion mutants as prey with or without 10^{-4} M GA_3. Right, β-Gal activity detected in a liquid assay with yeast strain Y187 transformants (means ± SD; $n = 3$). Left, Growth of yeast strain AH109 transformants on −His plates with or without 10^{-4} M GA_3.

higher peak fraction of SLR1 (M1-E104) contained SLR1 and GID1 proteins because these two proteins have similar MWs. In the case of Trx·His-SLR1 (M1-A172 ΔSPACE), we detected a peak from the GID1-SLR1 complex but also detected the individual peaks of GID1 and SLR1 as shoulders (Figure 5B, B-4). This result suggests that the complex of Trx·His-GID1 and Trx·His-SLR1 (M1-A172 ΔSPACE) is not as stable as the other complexes in vitro, even though high levels of β-Gal activity resulting from the interaction between SLR1 (ΔSPACE) and GID1 were found in yeast (Figure 4B). High levels of β-Gal activity by the SLR1 (ΔSPACE)–GID1 interaction in yeast may be caused by the C-terminal half of SLR1 because Trx·His-SLR1 (M1-A172 ΔSPACE) for the in vitro interaction experiment did not contain the C-terminal half, while the ΔSPACE construct for the Y2H experiment contained this region.

The results of the Y2H and in vitro interaction experiments demonstrate that the N-terminal portion of SLR1, including the DELLA and TVHYNP domains (M1-A172), is essential and sufficient for the GA-dependent GID1–SLR1 interaction. The requirement of both domains for their in vivo interaction was also demonstrated using BiFC experiment (Figure 1B). Moreover, the GA-dependent in vitro interaction between GID1 and SLR1 (M1-A172) strongly suggests that the interaction is a simple biochemical reaction that does not involve any other factors.

Domain Analysis of the GID1 Protein

We previously reported four *gid1* alleles, *gid1-1* to *-4*, all of which showed similarly severe dwarf phenotypes (Ueguchi-Tanaka et al., 2005). So far, we have isolated another four alleles, *gid1-5* to *-8* (Figure 6A). Two of these, *gid1-5* and *-6*, caused severe phenotypes resembling the *gid1* null allele, *gid1-4*, which contains a 302-bp internal deletion between intron 1 and exon 2 that produces a 492-nucleotide transcribed insertion containing a stop codon from the nonspliced intron 1 (Figure 6A). This result suggested that the products of these mutant alleles may completely lack activity. *gid1-5* and *-6* could not form any fertile flower similar to other severe mutant alleles, *gid1-1* to *-4*, as described previously (Ueguchi-Tanaka et al., 2005). By contrast, *gid1-7* and *-8* showed milder phenotypes. *gid1-8* homozygotes could produce flowers and seeds, whereas *gid1-7* homozygotes, which reached about half of the height of *gid1-8* and two to three times that of the other mutant alleles (Figure 6B), could not produce fertile flowers.

The mutations of the severe alleles, *gid1-1* to *-6*, are caused by deletions or replacement of amino acids that are conserved between rice and *Arabidopsis* GID1 proteins and that are located in the central part of GID1 (Figure 6A). The mutated proteins produced by these mutant *GID1* genes in *E. coli* showed no GA binding activity in vitro (Figure 6C). By contrast, the weak alleles, *gid1-7* and *-8*, have one amino acid deletion near the C-terminal end and a single amino acid change near the N terminus, respectively (Figure 6A). Both mutant proteins showed GA binding activity, with reduced levels in comparison to that of the intact GID1 protein (Figure 6C). The SLR1-interacting activity of these mutated GID1s was also investigated by Y2H assays (Figure 6D). GID1-1, -3, -5, and -6 showed no SLR1-interacting activity, as expected by their GA binding activities. GID1-2 showed a weak SLR1-interacting activity, detected only by a plate assay, a result consistent with the slightly milder phenotype of *gid1-2* compared with the more severe alleles (Ueguchi-Tanaka et al., 2005). Unexpectedly, however, GID1-7 and GID1-8 showed higher activities than the intact GID1, especially GID1-7, which had ~8 times higher activity than the intact protein. Therefore, the weak phenotypes of both alleles may not be explained only by weak GA binding activity or weak SLR1-interacting activity. It is not yet clear why the GID1-7 mutation, which results in high interacting activity with SLR1, causes the GA-insensitive phenotype. One possible explanation is that the much higher interacting activity of GID1-7 with SLR1 may prevent or interfere with the SLR1-GID2 interaction and SLR1 degradation.

To identify GID1 regions that are essential for GA binding, we produced a deletion series of GID1 in *E. coli* (Figure 6A) and

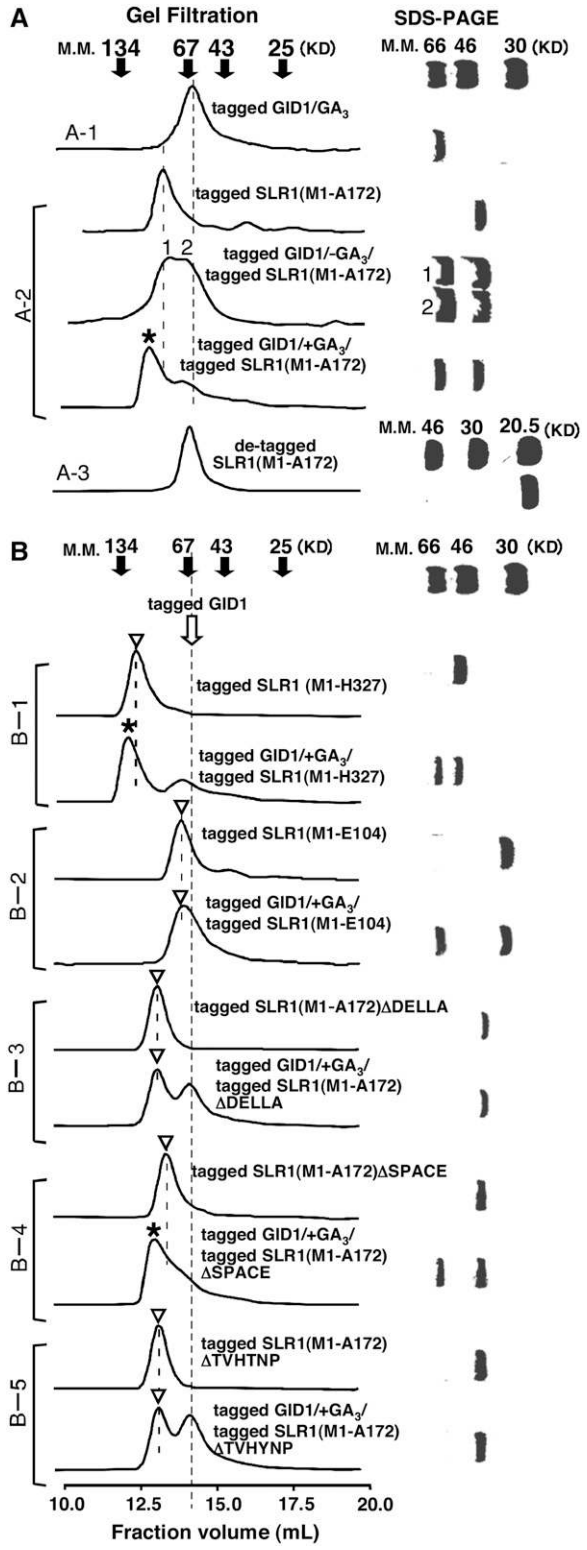

Figure 5. In Vitro Interaction between GID1 and SLR1 via DELLA and TVHYNP Domains.

(A) Left: elution profiles of Trx·His-GID1, Trx·His-SLR1(M1-A172), the mixture of Trx·His-GID1 and Trx·His-SLR1(M1-A172) in the absence or presence of 10^{-4} M GA_3, and detagged SLR1 (M1-A172) by Superdex-200 gel filtration. Trx·His-GID1 was eluted as a monomer, while SLR1 (M1-A172) with or without the tag was eluted at much larger MW fractions. The MW of the peak fractions was estimated from the following molecular markers (M.M.): 25-kD chymotrypsinogen A, 43-kD ovalbumin, 67-kD albumin, and 134-kD albumin dimer, which are indicated by arrowheads at the top. Dashed lines indicate the peak positions of Trx·His-SLR1 (M1-A172) (~85 kD) and Trx·His-GID1 (~65 kD). Peaks 1 and 2 indicate overlapping peaks of the mixture of Trx·His-GID1 and Trx·His-SLR1 (M1-A172) in the absence of GA_3. The asterisk indicates a new peak of the same mixture in the presence of GA_3 with disappearance of peaks 1 and 2. Each peak fraction was subjected to SDS-PAGE. Right: SDS-PAGE of each peak fraction.

(B) Left: elution profiles of various kinds of mutant Trx·His-SLR1s and their mixtures incubated with Trx·His-GID1 in the presence of 10^{-4} M GA_3 by Superdex-200 gel filtration. The tightly dashed line indicates the peak position of Trx·His-GID1 (tagged GID1; ~63 kD). The roughly dashed lines indicate the peak position of each Trx·His-SLR1 mutant protein. Peaks shifted by incubation with GID1 and GA_3 are indicated by asterisks, and peaks not shifted by incubation are indicated by open arrowheads. These peaks were subjected to SDS-PAGE. Right: SDS-PAGE of each peak fraction. The molecular marker for gel filtration and SDS-PAGE are the same as in **(A)**.

examined GA binding activities in vitro (Figure 6E). GA binding was reduced to ~25% of the activity of the full-sized GID1 protein when the 15 N-terminal amino acids (ΔN1) were deleted. Further deletion of 58 and 98 N-terminal residues (ΔN2 and ΔN3, respectively) caused complete loss of GA binding activity, as did the deletion of 30 C-terminal amino acids (ΔC). The SLR1-interacting activity of these deleted GID1s was also investigated by Y2H assays (Figure 6F). The results were essentially the same as those of the in vitro GA binding experiment. These results demonstrate that most parts of the GID1 protein, apart from the 15 N-terminal amino acids, are necessary for its activity. Otherwise, the protein structure and conformation of almost all of GID1 is important for its activity.

Next, we performed an Ala scanning experiment. We selected all conserved amino acid residues among the rice and three *Arabidopsis* GID1 proteins (see Supplemental Figure 3 online) and packed three or less contiguous conserved amino acids as one block. Then, these conserved amino acids in each block were exchanged with Ala residues. Consequently, we produced 94 mutagenized GID1 proteins carrying exchanged Ala residues in each conserved block (Figure 7). We used these mutagenized GID1s to analyze the GA binding and GA-dependent GID1–SLR1 interaction activities.

There were 12 blocks essential for GA binding activity (shown by hatched boxes in Figure 7A). These blocks were scattered throughout the GID1 molecule. This result is consistent with the above prediction that almost the entire GID1 protein is important for its GA binding activity. As previously mentioned, GID1 shares sequence similarity with the consensus sequence for the HSL family. When we draw attention to the residues shared with well-conserved motifs in the HSL family, the HGG and GXSXG motifs (indicated by HGG and GDSSG in Figure 7B, respectively) were also important for GA binding of GID1, but the last two residues of the GXSXG motif, S and G, were exchangeable with Ala without loss of GA binding activity. Furthermore, one of the conserved

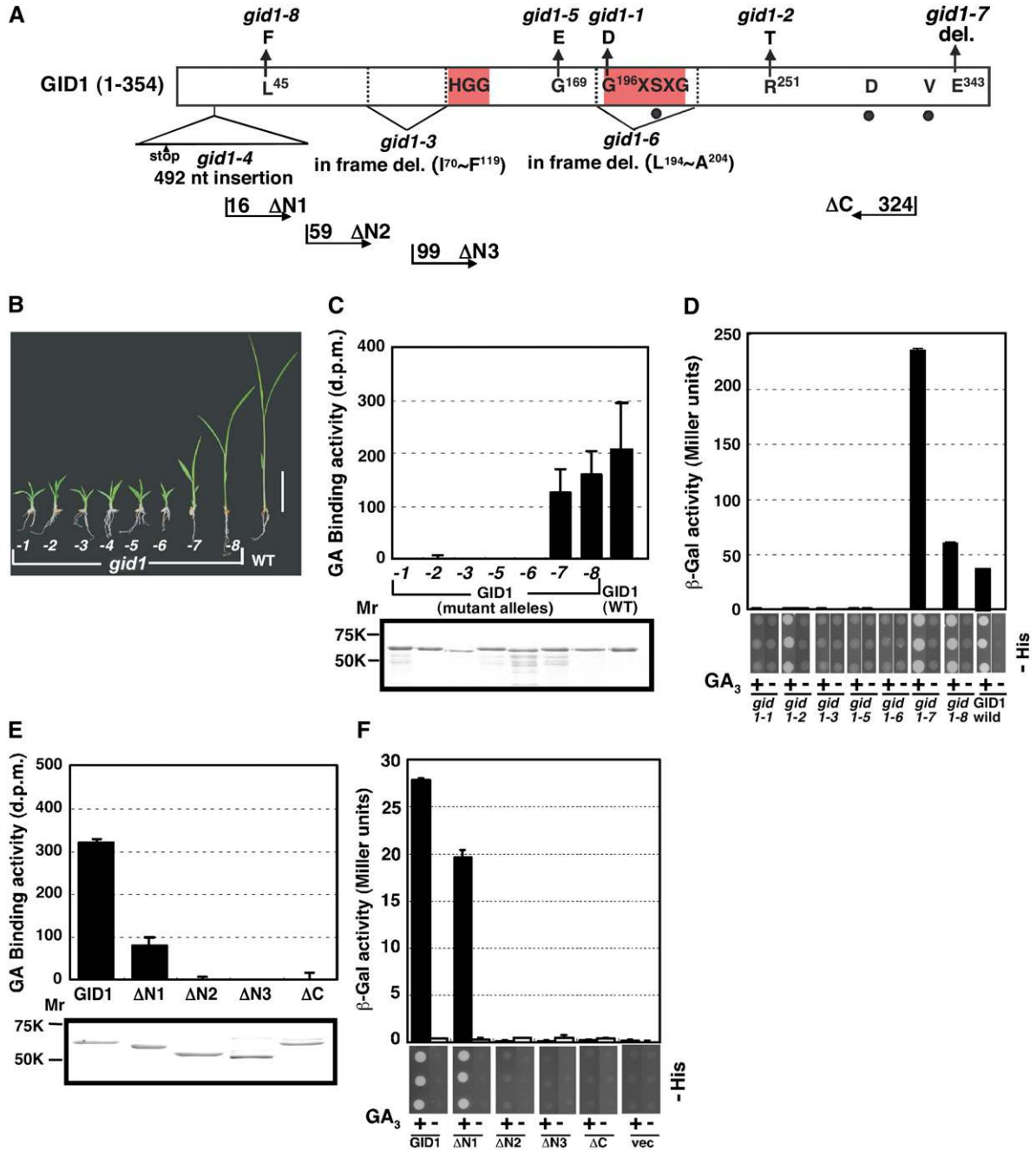

Figure 6. Eight *gid1* Mutant Alleles and GA Binding and SLR1-Interacting Activities of Mutated GID1 Proteins.

(A) A schematic structure of GID1 represents the mutation positions of eight *gid1* alleles and the positions of N-terminal (ΔN1, ΔN2, and ΔN3) and C-terminal (ΔC) deletions. Amino acid residues shared with HSL, such as HGG and GXSXG, are presented within red boxes. The residues corresponding to the catalytic triad of HSL, S, D, and V, are also presented by filled circles.

(B) Gross morphology of eight *gid1* mutant alleles grown for 2 weeks. A wild-type plant is shown as a control. Bar = 5 cm.

(C) Top: GA binding activities of Trx·His-GID1 (wild type) and the corresponding mutated *gid1* alleles. Data are means ± SD; $n = 3$. Bottom: Coomassie blue control. Approximately equal amounts of proteins (~3.2 μg) were used.

(D) Y2H assay using full-length GID1 and the corresponding mutated *gid1* alleles as baits and the full-length SLR1 as prey in the presence (+) and absence (−) of 10^{-4} M GA_3. The Y2H assay was performed the same as in Figure 4B. Top: β-Gal activity (means ± SD; $n = 3$). Bottom: growth of yeast on −His plates.

(E) Top: GA binding activities of Trx·His-GID1 and mutated Trx·His-GID1s with deletions in the N-terminal (ΔN1, ΔN2, and ΔN3) or C-terminal (ΔC) regions. Data are means ± SD; $n = 3$. Bottom: Coomassie blue control. Approximately equal amounts of proteins (~3.2 μg) were used.

(F) Y2H assay using full-length GID1 and mutated GID1s with deletions in the N-terminal (ΔN1, ΔN2, and ΔN3) or C-terminal (ΔC) regions as baits and the full-length SLR1 as prey in the presence (+) and absence (−) of 10^{-4} M GA_3. The Y2H assay was performed the same as in Figure 4B. Top: β-Gal activity (means ± SD; $n = 3$). Bottom: growth of yeast on −His plates.

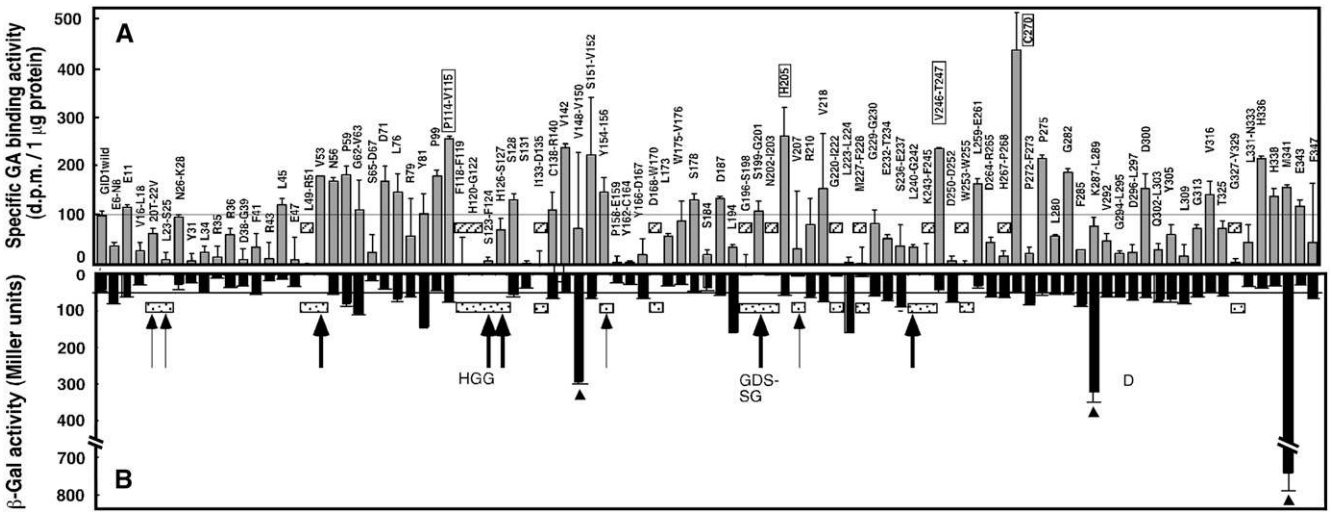

Figure 7. Ala Scanning Analysis of GID1 for Its GA Binding and SLR1-Interacting Activities.

(A) Specific GA binding activity of 94 mutated Trx·His-GID1s and wild-type Trx·His-GID1 (at the left). Mutated residues are indicated at the top of each bar. Specific activity was calculated as radioactivity (dpm) per microgram of protein. Data are means ± SD; $n = 3$. Hatched boxes indicate the mutant proteins showing no GA binding activity. The mutated proteins showing increased activity that are discussed in the text are boxed.

(B) SLR-interacting activity of 94 mutated GID1s and the wild-type GID1 (at the left). Y2H assay using 94 mutated and wild-type GID1s as baits and the full-length SLR1 as prey in the presence of 10^{-4} M GA_3. Each mutation of GID1 corresponds to **(A)**. Dotted boxes indicate the mutant proteins showing no β-Gal activity. Thick and narrow arrows indicate mutant proteins having GA binding activity but not SLR1-interacting activity, whose mutation points are adjacent to the hatched box (thick) or independently located (narrow). The mutated proteins having increased SLR1-interacting activity that are discussed in the text are indicated by arrowheads. HGG and GDSSG correspond to the substrate binding pocket of HSL, and D corresponds to one of the residues in the catalytic triad in HSL.

amino acid residues forming the catalytic triad of HSL, D^{296} (indicated by D in Figure 7B), was also exchangeable with Ala. These results demonstrate that not all the conserved regions shared with HSL proteins are important for GA binding activity.

There were 13 blocks important for GID1–SLR1 interaction (shown by dotted boxes in Figure 7B). All regions essential for GA binding were included in these blocks, confirming that GA binding to GID1 is a prerequisite for GID1–SLR1 interaction. On the other hand, there are eight blocks that carried GA binding but not GID1–SLR1 interaction activity (shown by arrows in Figure 7B). These regions are considered to be involved in the interaction with SLR1 but not necessary for GA binding. These eight blocks are classified into two groups, that is, one is adjacent to the region essential for GA binding (indicated by thick arrows), and another is located independently from any other region (indicated by narrow arrows). Such high proximity to the regions essential for SLR1 interaction and GA binding suggests that GA binding and SLR1 interaction may be overlapping on the GID1 molecule. Some Ala exchanges increased the GA binding activity. For example, exchange of Cys-270 caused ~4 times higher GA binding activity relative to the intact GID1 (indicated by boxes in Figure 7A). Some residues, whose replacement also caused higher GA binding activity, such as Pro-114–Val-115, His-205, and Val-246–Thr-247, are adjacent to regions essential for GA binding (indicated by boxes in Figure 7A). Similarly, a few Ala exchanges, such as Val-148–Val-150, Lys-287–Leu-289, and Met-341 (indicated by arrowheads in Figure 7B), caused higher GID1–SLR1 interaction, yet these replacements did not affect their GA binding activity. This result indicates that higher GID1–SLR1 interaction by these exchanges is not due to increased GA binding but is due to increased interaction between GID1 and SLR1. Such a phenomenon was also seen in the GID1-7 mutant protein, namely, this mutant GID1 protein showed >8 times higher interaction activity with SLR1 relative to the wild-type GID1 without increasing its GA binding activity (Figures 6C and 6D). It is noteworthy that the mutation site of *gid1-7* is located at Glu-343, a one–amino acid deletion, whereas the Ala exchange at Met-341 caused a >10 times increase in the GID1–SLR1 interaction. Taken together, it is possible that there is a hot spot region around Met-341–Glu-343 involving the formation and/or stability of the GID1-SLR1 complex.

Structure-Function Relationship of GID1

The Ala scanning experiment revealed that the amino acid residues essential for these activities are scattered throughout the GID1 molecule. We expected that such irregular placement of the important residues is reflected in the stereostructure of GID1. Therefore, we predicted the secondary structure of GID1 by the Jpred program (Cuff et al., 1998) (Figure 8A). As described previously, the primary structure of GID1 resembles that of proteins in the HSL group. To date, the secondary and tertiary structures of three bacterial esterases in the HSL family, Brefeldin A esterase, *Archaeoglobus fulgidus* esterase (AFEST), and *Alicyclobacillus acidocaldarius* esterase 2 (EST2), have been characterized by the x-ray diffraction analyses (Wei et al., 1999;

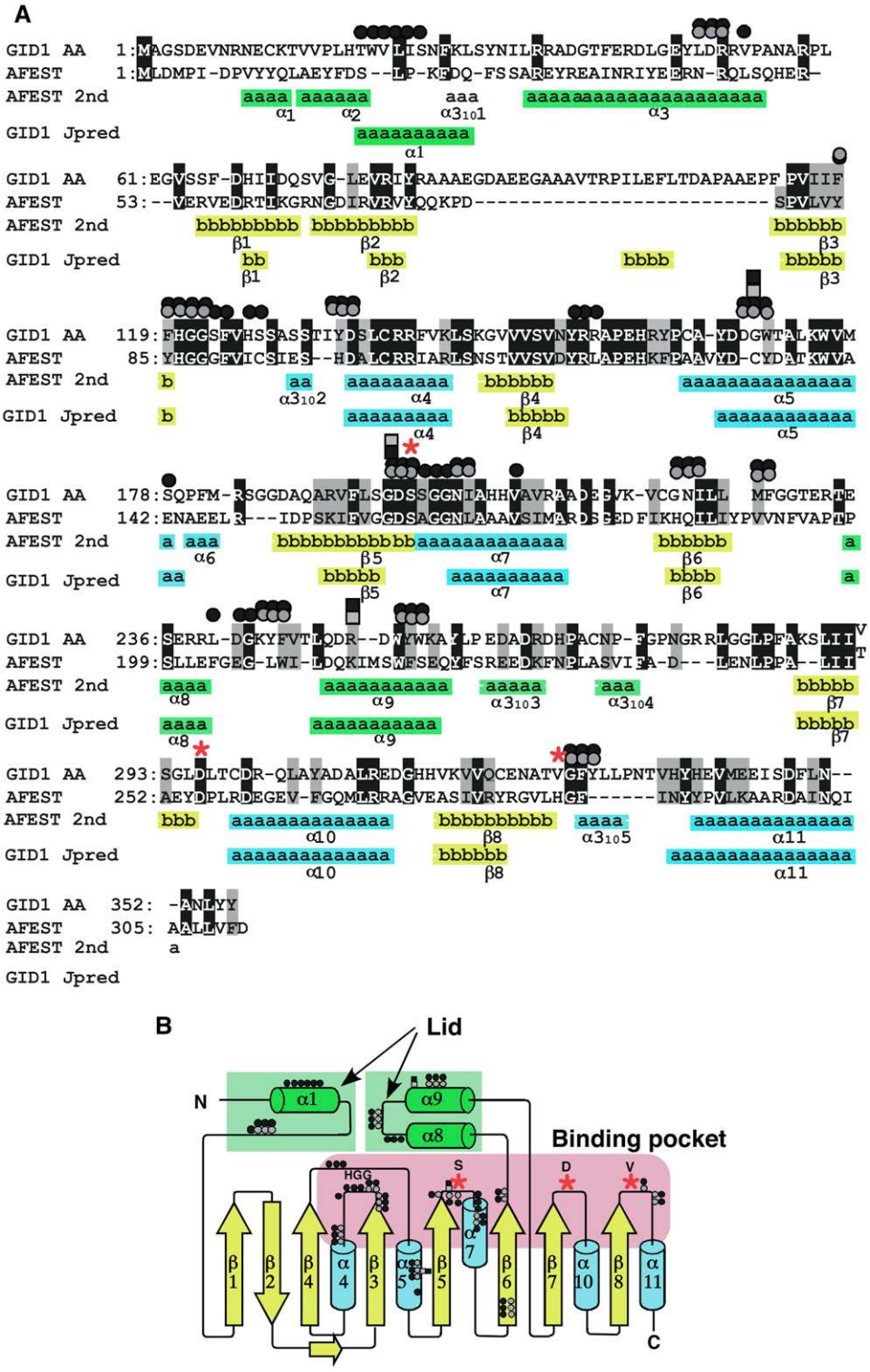

Figure 8. Prediction of the GID1 Secondary Structure, Location of Important Residues for GA Binding, and SLR1 Interaction Activity on the Predicted Structure.

(A) The alignment of GID1 and a member of HSL, AFEST, whose special conformation was analyzed by x-ray crystallography. The line of AFEST 2nd shows the secondary structure of AFEST analyzed by x-ray crystallography (De Simone et al., 2001). The predicted second structure of GID1 (GID1 Jpred) was calculated by a Jpred program (Cuff et al., 1998). α-helices and β-sheets are represented by a and b, respectively. Number of α-helices and

De Simone et al., 2000, 2001). The stereostructures of these proteins are similar to each other; therefore, proteins belonging to the HSL family have been considered to form a similar spatial conformation. Thus, based on an analogy between GID1 and AFEST, we compared a secondary structure of AFEST (AFEST 2nd in Figure 8A; De Simone et al., 2001) with the predicted secondary structure of GID1 (GID1 Jpred in Figure 8A). The structures of AFEST and the predicted GID1 are quite similar to each other with the exception of the N-terminal region that corresponds to the lid region known as a variable region in proteins of the HSL family. Most notably, the skeletal structure of HSL, composed with the canonical α/β hydrolase fold consisting of a parallel β-sheet surrounded on both sides by α-helices, is completely shared with the predicted structure of GID1. Furthermore, the predicted structure of GID1 contains two α-helices between β6 and β7 sheets (Figure 8B), corresponding to the right side of the lid structure, whereas the left side of the lid corresponds to the N-terminal region based on an analogy with the HSL structure. Thus, it is very possible that GID1 has the canonical α/β hydrolase fold with the lid structures similar to the HSL group proteins (Figure 8B). For enzymatic activity of HSL, the conserved HGG and catalytic triad, S, D, and H, are spatially located in close proximity to form a substrate binding pocket and catalytic site, respectively (Naridini and Dijkstra, 1999). In the predicted structure of GID1, the amino acids corresponding to these residues are located in close proximity at the upper side loops, while one amino acid of the catalytic triad, H, in HSL is replaced with V in GID1.

Then, we positioned the amino acid residues important for GA binding (black dots and squares identified by Ala scanning and spontaneous mutants, respectively) and SLR1-interacting activity (gray dots and squares identified by Ala scanning and spontaneous mutants, respectively) on this predicted structure of GID1 (Figure 8B). Interestingly, many residues important for GA binding and for SLR1 interaction are localized around the regions corresponding to the substrate binding pocket and lid regions in HSL. The lid structure of HSL is known to be involved in substrate specificity since it is moveable (Naridini and Dijkstra, 1999). Preferential localization of these amino acid residues in the substrate binding pocket and lid regions leads us to speculate that GID1 may interact with GA and SLR1 at this substrate binding pocket region in collaboration with the lid region in a similar fashion to HSL substrate interaction.

Stabilization of GA Binding to GID1 by SLR1

The possibility of overlapping SLR1-interacting and GA binding domains on the GID1 molecule led us to speculate that the binding properties between GID1 and GA may be affected by SLR1. Therefore, we compared the GA binding activity of GID1 with and without SLR1. The GA binding activity of Trx·His-GID1 was enhanced approximately threefold by GST-SLR1, whereas the GST tag alone was ineffective and GST-SLR1 alone did not show any GA binding (Figure 9A). We also measured the association and dissociation rates between Trx·His-GID1 and ^{3}H-16,17-dihydro-GA$_4$ (Figures 9B and 9C). Although the half-time of the association was not affected by GST-SLR1 (Figure 9B), the dissociation rate markedly increased in the presence of GST-SLR1 (Figure 9C). These results support the above idea that the interaction between GID1 and GA is stabilized by SLR1. These results also support the possibility that GA binding with GID1 may induce the SLR1 interaction with GID1; in turn, the interacting SLR1 covers the GA bound to GID1 and stabilizes the GID1–GA interaction (see Discussion).

DISCUSSION

In this article, we have studied the molecular mechanism for GA binding to GID1 and the mechanism of the GA-dependent interaction between GID1 and SLR1 protein. For this purpose, we used a Y2H assay because of its ease and reliability. To demonstrate the validity of this Y2H assay, we examined the in vivo GA-dependent GID1–SLR1 interaction by in vivo pull-down (Figure 1A) and BiFC experiments (Figure 1B). We also compared the GA selectivity of GID1 determined by the GID1–SLR1 interaction in yeast cells and the GA effectiveness in leaf sheath elongation to SLR1 degradation in rice seedling and callus (Figures 2 and 3). These results confirmed that the GA-dependent GID1–SLR1 interaction in yeast is reflective of the GA-dependent events occurring in rice plants.

The consistency in GA selectivity and GA dose dependency determined by the three different experiments, in vitro GA binding of GID1 (Ueguchi-Tanaka et al., 2005), Y2H assay monitoring the GID1–SLR1 interaction, and GA-dependent events occurring in rice plants, indicates that GA actions in rice cells are quantitatively and qualitatively reflected by the biochemical properties of the GID1 molecule through its quantitative interaction with SLR1.

GA Preference of GID1

The GA selectivity of GID1 determined by Y2H and the GA effectiveness to SLR1 degradation in rice seedling and callus demonstrated that GA$_4$ is the most favored GA, although GA$_4$ was not the most effective GA for leaf sheath elongation probably because of its rapid inactivation by GA-catabolizing enzymes. Our recent results demonstrate that the GA preference of three *Arabidopsis* GA receptors, At GID1s, is similar to that of rice GID1 (Nakajima, et al., 2006). Similar GA preference between rice and *Arabidopsis* GID1s suggests that the GID1 proteins both in monocot and dicot plants, and therefore perhaps all GID1s, may

Figure 8. (continued).

β-sheets of the predicted GID1 was according to that of AFEST 2nd. Essential residues for GA binding (gray) and SLR1 interaction (black) were determined by an Ala scanning experiment (dot) or spontaneous mutants, *gid1-1* (G^{196}→D), *gid1-2* (R^{251}→T), and *gid1-5* (G^{169}→E) (square). Three amino acid residues corresponding to the catalytic triad of HSL are represented as asterisks.

(B) A topology diagram of GID1 written by the predicted second structure in **(A)**. Symbols are the same as in **(A)**. The regions of the lid and binding pocket described in text are colored in light green and pink, respectively.

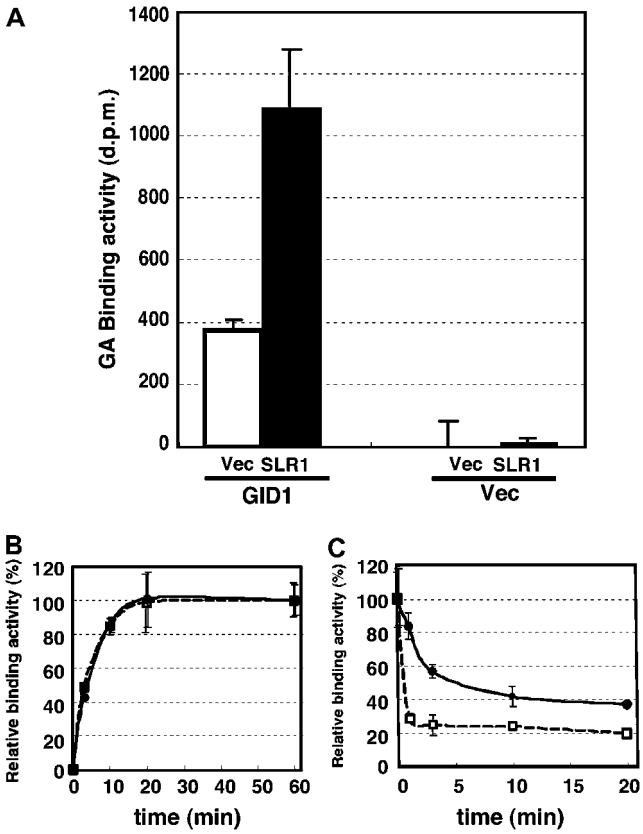

Figure 9. GA Binding Activity of GID1 Is Enhanced by SLR1.

(A) GA binding activity of Trx·His-GID1 with (black) and without (white) the full length of GST-SLR1 protein (means ± SD; $n = 3$). Approximately equal amounts of proteins (~3.2 μg) of Trx·His-GID1, Trx·His vec, GST-SLR1, and GST vector were used.

(B) Association kinetics of ^{3}H-16,17-dihydro-GA$_4$ and Trx·His-GID1 with (closed symbols) and without (open symbols) the full length of GST-SLR1, represented as percentage of the values reached after 60 min of reaction. Data are means ± SD; $n = 3$.

(C) Dissociation kinetics of ^{3}H-16,17-dihydro-GA$_4$ and Trx·His-GID1 with (closed symbols) or without (open symbols) GST-SLR1, represented as a percentage of the value detected at 0 min. Data are means ± SD; $n = 3$.

have similar GA preferences. If so, it is curious that the major bioactive GA is different in each plant species. For example, rice uses GA$_1$ as the major bioactive GA at the vegetative stage, whereas *Arabidopsis* uses GA$_4$. In the case of rice, the major bioactive GA also depends on its developmental stages. In the vegetative stage of rice, GA$_1$ is the major GA, while, in the reproductive stage, the amount of endogenous GA$_4$ is precisely regulated by the developmental stage (Luo et al., 2006; Zhu et al., 2006). For example, in pollen, an extremely high amount of GA$_4$ accumulates (Kobayashi et al., 1988). Since drastic GA-dependent reactions, such as rapid elongation of the heading stem and pollen tube, occur during the reproductive stage, rice may use the most effective GA at this stage and use GA$_1$ for ordinary GA-dependent reactions at the vegetative stage. Further studies will be necessary to explain this curious discrepancy between the common GA preference of GID1 and the choice of major bioactive GA in various plant species.

Domain Analysis of SLR1 Protein

The results of the Y2H assays (Figure 4) and in vitro interaction experiments (Figure 5) clearly demonstrate that the N-terminal portion of SLR1, including the DELLA and TVHYNP domains, is essential and sufficient for the GA-dependent GID1–SLR1 interaction. Moreover, we showed by the BiFC experiment that these domains are also necessary for in vivo GA-dependent interaction between GID1 and SLR1 (Figure 1B). Recently, two groups performed Y2H experiments using *Arabidopsis* DELLA proteins and At GID1a, with inconsistent results (Griffiths et al., 2006; Willige et al., 2007). Griffiths et al. (2006) reported that the DELLA and VHYNP domains of RGA are both necessary for At GID1a binding, whereas Willige et al. (2007) reported that the VHYNP domain of GAI is not needed for GA-dependent At GID1a interaction and proposed that the DELLA domain functions as a receiver domain for the GA receptor. Our results from using truncated versions of SLR1 are consisted with the observations of Griffiths et al. (2006) with RGA. It is an interesting possibility that there might be two different types of DELLA proteins in plants: one type, such as SLR1 and RGA, requiring both the DELLA and TVHYNP/VHYNP domains for GID1 interaction, and the other, including GAI, requiring only the DELLA domain. Further studies, using not only Y2H assays but also in vitro and in vivo interaction experiments, will be necessary to identify the domain(s) of DELLA proteins that is essential for GID1 interaction in *Arabidopsis* and other plants.

Domain Analysis of the GID1 Protein and a Model of the GID1-GA-SLR1 complex

By comparing the Ala scanning analysis of GID1 and the mutation analysis of *gid1* alleles with the GID1 structure predicted by analogy with the HSL tertiary structure, it appeared that many residues important for GA binding and for SLR1 interaction are localized around the regions corresponding to the substrate binding pocket and lid regions in HSL. Based on these results, we predicted the interacting model of the GID1-GA-SLR1 complex (Figure 10). In this model, the structure of the GID1 receptor resembles those of the HSL proteins. GID1 has the regions

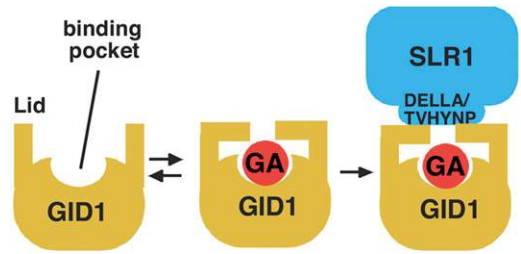

Figure 10. Molecular Model for Formation of the GA-GID1-SLR1 Complex.

See text for details.

corresponding to the substrate binding pocket and lid like the bacterial HSLs. Similarly to the mechanism for substrate binding in other HSLs, GID1 binds GA within the binding pocket with the aid of the lid. SLR1 interacts with the GID1-GA complex at its N-terminal region, including the DELLA and TVHYNP domains. Both the lid and the binding pocket containing GA are necessary for the SLR1 interaction, and as a result of SLR1 binding, the GID1-GA complex is stabilized.

Our results showing the stabilization of the GA–GID1 interaction by SLR1 (Figure 9C) strongly support this model and suggest that the interaction of SLR1 with GA-GID1 might close the lid, thereby ensuring that GA will be held in the substrate pocket. The stabilized complex of GA, GID1, and SLR1 may be targeted by GID2, an F-box protein, leading to its degradation by 26S proteasomes through ubiquitination of the SCF^{GID2} complex. In fact, recent results from Y3H assays indicated that the GA-GID1 complex promoted the interaction between an *Arabidopsis* DELLA protein, RGA, and an F-box protein, SLY1 (Griffiths et al., 2006). Further studies, including a structural analysis of GID1, are necessary to support this model.

METHODS

Plant Materials, Growth Conditions, and Screening of the *gid1* Mutant Alleles

The new alleles of *gid1* were obtained by screening three rice (*Oryza sativa*) libraries mutagenized by γ-irradiation, by cell culture followed by regeneration, and by *N*-methyl-*N*-nitrosourea. We first screened GA-related mutants showing dwarfism and wide dark-green leaves. Then, GA-insensitive mutants were screened by the GA treatment. After sequencing the *GID1* gene, we found four new alleles: *gid1-5*, from *O. sativa* cv Nipponbare mutagenized by γ-irradiation; *gid1-6* and *gid1-7* from *O. sativa* cv Nipponbare mutagenized by cell culture; and *gid1-8* from *O. sativa* cv Taichung 65 mutagenized by *N*-methyl-*N*-nitrosourea. Rice plants were grown in a greenhouse at 30°C (day) and 24°C (night).

GA Treatment of Rice Seedlings and Callus

For the GA response tests by a one-drop treatment, sterilized *Tan-Ginbozu* seeds (Itoh et al., 2004) were germinated on solid half-strength Murashige and Skoog medium. After 2 d, 1 μL of GA (10^{-6}, 10^{-5}, 10^{-4}, and 10^{-3} M; in 50% acetone) was added to the joint between the coleoptile and leaf sheath of each seedling. For the control, 1 μL of 50% acetone was added. The length of the second leaf sheaths was measured 6 d later. For the GA dose–response tests, sterilized seeds of *Tan-Ginbozu* (Itoh et al., 2004) were germinated in various concentrations of GA solution and the length of the second leaf sheaths was measured 8 d later. Young seedlings that had been grown in the greenhouse for 2 weeks were used for the detection of GA-dependent degradation of the SLR1 protein in shoots. Old leaves were removed so that the seedling retained only the newest leaf blade and sheath and the second newest leaf sheath. The seedlings were incubated in various concentrations of GA solution containing 0.02% Tween 20 for 2 h at room temperature with gentle shaking. For the control, 0.1% ethanol solution containing 0.02% Tween 20 was used. After 2 h, the seedlings were collected and frozen at −80°C until used for protein gel blot analysis. Callus of wild-type rice (Taichung 65) was used for the detection of GA-dependent degradation of the SLR1 protein in callus. The callus was transferred to new N6D solid medium. After 3 d, the callus was treated with various concentrations of GA solution, containing 0.02% Tween 20, for 5 min at room temperature. The callus was then immediately frozen at −80°C until it was used for protein gel blot analysis.

Plasmid Construction

Sequences of primers used in this study are listed in Supplemental Table 1 online. The PCR fragments were sequenced to confirm that no mutations were induced. For the Y2H assay, pGADT7 (Clontech) and pGBKT7 (Clontech) were used as expression vectors. The mutated *GID1* fragment corresponding to *gid1-1*, *-2*, *-3*, *-5*, *-6*, *-7*, and *-8* were produced by RT-PCR using total RNA from seedlings of *gid1* mutant alleles, with Y2H/GID1f and Y2H/GID1r primers, and cloned into the *Nco*I-*Sma*I site of the pGBKT7 vector. The fragments corresponding to the N-terminal and C-terminal deletions of GID1 were produced by PCR with appropriate primers having *Nco*I and *Sma*I sites and cloned into the *Nco*I-*Sma*I site of the pGBKT7 vector. The fragments for internal deletions of SLR1, ΔDELLA, ΔSPACE, ΔTVHYNP, ΔpolyS/T/V, and ΔLZ, were produced by PCR using a corresponding deletion series of SLR1 cDNA, previously made in a binary vector (Itoh et al., 2002), as templates with Y2H-SLR1f and Y2H-SLR1r primers and cloned into the *Nde*I-*Eco*RI site of the pGADT7 vector. The fragments for the C-terminal deletion of SLR1, M1-H327, M1-A172, and M1-E104, were produced by PCR with Y2H-SLR1f and appropriate reverse primers and cloned into the *Nde*I-*Eco*RI sites of pGADT7. A full-length *GID1* cDNA inserted into the pGBKT7 vector and a full-length *SLR1* cDNA inserted in the pGADT7 vector were described previously (Ueguchi-Tanaka et al., 2005).

To construct Trx·His tagged proteins, except for the Ala-exchanged Trx·His -GID1 protein, we used the pDEST·Trx vector that is derived from pET32a (Novagen) for the Gateway system (Tsunoda et al., 2005). The PCR fragments, amplified with primers having a appropriate site for the Gateway system were cloned into the entry vector of pENTR/SD/D-TOPO (Invitrogen) and recombined into the destination vector of pDEST·Trx according to the Gateway instruction manual (Invitrogen). For the construction of the mutated Trx·His-GID1s and the mutated GID1s in the pGBKT7 vector for the Ala scanning experiment, a full-length wild-type *GID1* was amplified with GID1Alaf and GID1Alar primers and cloned into the pCR4 Blunt-TOPO vector. Then, PCR was performed against the full-length GID1 cDNA with one set of mutagenized primers corresponding to each mutation. The parental methylated and hemimethylated DNA in the PCR reaction mixture was digested with *Dpn*I, and the mutated GID1 cDNA that could not be digested with *Dpn*I was transformed into *Escherichia coli* XL10-Gold (Stratagene). After sequencing, each mutated GID1 cDNA was digested with *Nco*I-*Eco*RI or *Bam*HI-*Hin*dIII and cloned into pGBKT7 and the pET32a vector, respectively. For construction of *GST-SLR1*, the cDNA was inserted into the pGEX-4T vector (GE Healthcare) at the *Eco*RI target site. For the construction of GFP-GID1 in the pActNos/Hm2 vector, the GFP fragment was amplified using the GFP cDNA as a template and the GFP-f and GFP-r primers and inserted into the GID1 cDNA at the *Nco*I target site, which is located just before the initial ATG codon. The GFP-GID1 construct was digested with *Sma*I and cloned into pActNos/Hm2 at the *Sma*I target site. For the insertion of GFP-GID1 into the pET32a vector, the 2.0-kb GFP-GID1 fragment was amplified using the pActNos/Hm2 construct described above as a template and the GFP-GID1-f and GFP-GID1-r primers. The fragment was cloned into pCR4 Blunt-TOPO (Invitrogen), generating GFP-GID1/pCR4 Blunt-TOPO. The GFP-GID1 fragment was then removed from GFP-GID1/pCR4 Blunt-TOPO by digestion with *Bam*HI and *Hin*dIII and then inserted into the pET32a vector at the *Bam*HI and *Hin*dIII target sites.

For constructs used in the BiFC experiment, the N-terminal half of the EYFP clone without a stop codon and the C-terminal half of the EYFP clone without a stop codon were kindly provided by T. Araki. To construct N·EYFP-GID1 (NY-GID1), the 0.5-kb fragment of the N-terminal half of EYFP was produced using the N-terminal half of the EYFP clone without a stop codon as a template with BiFC-5 and BiFC-6 primers and cloned into the *Xba*I-*Sma*I site of the pUC18 vector (Takara), generating NY/pUC18. The 1.2-kb fragment of GID1 was produced using a full-length *GID1* cDNA as a template with BiFC-15 and BiFC-16 primers and cloned into pCR4 Blunt-TOPO (Invitrogen), generating BiFC-GID1. NY/pUC18 was digested

with *Sma*I and *Sac*I and ligated to a 1.2-kb *Sma*I-*Sac*I fragment of BiFC-GID1 to generate NY-GID1/pUC18. NY-GID1/pUC18 was digested with *Xba*I and *Sac*I, and the 1.7-kb *Xba*I-*Sac*I fragment was inserted into the *Xba*I-*Sac*I site of pBI121 (Toyobo), generating NY-GID1. To construct the C·EYFP-SLR1s (CY-SLR1s) containing full-length or truncated SLR1, the 0.3-kb fragment of the C-terminal half of EYFP was produced using the C-terminal half of the EYFP clone without a stop codon as a template with BiFC-7 and BiFC-8 primers and cloned into the *Xba*I-*Sma*I site of the pBluescript II SK+ vector (Stratagene), generating CY/pBS. The SLR1, ΔDELLA-SLR1, and ΔTVHYNP-SLR1 fragments were amplified from a full-length *SLR1* cDNA, or corresponding truncated SLR1s in the pGADT7 vector, using the BiFC-13 and BiFC-14 primers. The fragments were cloned into the pCR4 Blunt-TOPO vector, generating the BiFC-SLR1s. CY/pBS was digested with *Sma*I, and the CY fragment was ligated to the *Sma*I fragment of the BiFC-SLR1s in the correct orientation, generating CY-SLR1s/pBS. pBI121 was digested with *Sac*I, blunted with T4 DNA polymerase (Takara), and digested with *Xba*I. *Xba*I-*Eco*RV fragments from the CY-SLR1/pBS plasmids were inserted into pBI121 at the *Xba*I and blunt-end *Sac*I sites to generate the CY-SLR1s.

Production of Recombinant Protein

E. coli BL21 (DE3) pLysS Rosseta-gami 2 (Novagen) was used as a host strain for the production of each recombinant protein. To produce recombinant Trx·His-GIDs for use in GA binding assays, 5 mL of precultured cells were added to 500 mL of Luria-Bertani (LB) medium in a 2-liter flask, or 1.5 mL of precultured cells were added to 150 mL of LB medium in a 500-mL flask for the Ala scanning experiment and cultured at 37°C until OD_{600} 0.4 to 0.6. Recombinant proteins were induced by the addition of 0.01 mM isopropyl-β-D-thiogalactopyranoside (IPTG) and further incubated at 18°C for 18 h. Cells were harvested and resuspended with buffer A containing 50 mM Tris-HCl, pH 8.0, 100 mM NaCl, 10 mM imidazole, and 0.1% Triton X-100. The cells were lysed by sonication (20 kHz, 5 s × 40 times). Or for the Ala scanning experiment, the cells were lysed by addition of the detergent BugBuster protein extraction reagent (Novagen) with benzonase nuclease (Benzon Pharma) according to the instruction manual. Each lysate was centrifuged at 16,000*g* for 30 min, and the supernatants were mixed usually with 400 or 100 μL (for the Ala scanning experiment) of TALON metal affinity resin (Clontech) and rotated for 2 h at 4°C. The resin was washed five times with buffer A and eluted five times with 400 μL usually or 100 μL (for the Ala scanning experiment) of 500 mM imidazole in buffer A. The five eluates were pooled and desalted using a PD-10 column (GE Healthcare) equilibrated with buffer B containing 20 mM Tris-HCl, pH 7.5, 0.15 M NaCl, and 2 mM 2-mercaptoethanol (2-ME) or dialyzed against 2 liters of buffer B (for the Ala scanning experiment) for 18 h. For production of recombinant Trx·His-GIDs for use in the gel filtration analyses, the cell culture and induction were performed the same as the recombinant Trx·His-GIDs for the GA binding assays; however, a different purification method was used because the gel filtration analysis needed more highly purified proteins. Cells were harvested and resuspended with buffer C containing 20 mM Tris-HCl, pH 7.5, 0.5 M NaCl, and 2 mM 2-ME. The cells were lysed by sonication (20 kHz, 10 s × 20 times), the lysates were centrifuged at 16,000*g* for 30 min, and the supernatants were loaded directly onto 5 mL of Ni-chelating HP (GE Healthcare) equilibrated with buffer C and eluted by increasing the imidazole concentration to 0.5 M at a flow rate of 5 mL per min. The eluate was dialyzed against buffer C and loaded onto a Hi-Load 26/60 Superdex 200 pg column (GE Healthcare). Purified recombinant proteins were analyzed by immunoblotting. The production method for recombinant Trx·His-SLR1s to use in gel filtration analyses was the same as for Trx·His-GID1 used for gel filtration analysis. Purified recombinant proteins were analyzed by immunoblotting and subjected to matrix-assisted laser desorption ionization–time of flight–mass spectrometry for measurement of MW.

For the production of recombinant GST and full-length GST-SLR1, the cell culture and induction were performed the same as Trx·His-GID1 for the GA binding experiment, except 0.4 mM IPTG was used instead of 0.01 mM IPTG. Cells were harvested and resuspended with buffer D containing 50 mM Tris-HCl, pH 8.0, 50 mM NaCl, 1 mM EDTA, and 1 mM DTT. The cells were lysed by sonication (20 kHz, 5 s × 40 times) with 1% Triton X-100. The lysates were centrifuged at 16,000*g* for 30 min, and the supernatants were mixed with 2 mL of Glutathione Sepharose 4B beads (GE Healthcare) and rotated for 2 h at 4°C. The beads were washed five times with PBS containing 1% Triton X-100 and eluted five times with 400 μL of 20 mM glutathione in buffer D. The five eluates were pooled and desalted using a PD-10 column (GE Healthcare) equilibrated with buffer E containing 20 mM Tris-HCl, pH 7.5, and 2 mM 2-ME and further purified by a MonoQ 5/50 GL (GE Healthcare) column equilibrated with buffer E and eluted by increasing the NaCl concentration to 0.5 M at a flow rate of 0.5 mL per min. The peak fraction corresponding to full-length GST-SLR1 was collected, identified by immunoblotting, and used for in vitro binding experiments.

GA Binding Assay

In vitro assays for GA binding were performed as described previously except that Trx·His-GID1 and its derivatives were used instead of GST-GID1 that was used in the previous article (Ueguchi-Tanaka et al., 2005). The GA binding activity of Trx·His-GID1 was almost the same as that of GST-GID1 in vitro (data not shown). In the case of the Ala scanning experiment, 100 μL of each mutated Trx·His-GID1 in buffer B was added to 300 μL of reaction mixture. The amount of each mutated protein was determined from the band intensity of SDS-PAGE using 0.25, 1, and 4 μg of BSA as a quantity standard (see Supplemental Figure 3 online), and the GA binding activity was represented as a radioactivity (dpm) per microgram of protein. For quantification of the protein from the SDS-PAGE profile, NIH Image software was used.

The effect of SLR1 on GA binding of GID1 was studied by a GA binding assay. Purified Trx·His-GID1 proteins were dissolved in 200 μL binding buffer (20 mM Tris-HCl, pH 7.6, 0.1 M NaCl, and 2 mM 2-ME) and incubated with ^{3}H-16,17-dihydro-GA_4 (6 pmol) either without excess unlabeled GA_4 for total binding or with an 833-fold excess of unlabeled GA_4 for nonspecific binding. The total volume of the reaction mixture was 300 μL. After 15 min of incubation, 100 μL of GST-SLR1 proteins were added to each reaction tube. After incubation for 45 min, radioactivity of the tritiated 16,17-dihydro-GA_4 bound to GST-GID1 was measured. As a control, GST protein produced from the empty GST vector was added instead of GST-SLR1.

To determine the association rate of GA binding, purified Trx·His-GID1 proteins (16 μg) were dissolved in 250 μL of binding buffer; 100 μL of the purified GST-SLR1 (16 μg) or the vector control (GST) were added, and the solution was incubated with 50 μL of ^{3}H-16,17-dihydro-GA_4 (6 pmol) for various periods. For measurement of the dissociation rate of GA binding, the association reaction was performed for 20 min before an 833-fold excess of unlabeled GA_4 was added, followed by incubation for various periods. After incubation, radioactivity of the tritiated 16,17-dihydro-GA_4 bound to Trx·His-GID1 was measured.

Y2H Assay and Pull-Down Assay

The Y2H assay was performed as described previously (Ueguchi-Tanaka et al., 2005). The yeast strain Y187 was used for detection of β-Gal activity by liquid assay, and the strain AH109 was used for growth tests on −His plates with or without GA. The basis for the pull-down assay was to detect if SLR1-GST could bind Trx·His-GID1 that was immobilized on TALON metal affinity resin. For the pull-down assay, 2 μg of Trx·His-GID1 was incubated with 1 μg of GST-SLR1 at 30°C for 15 min in 300 μL of binding

buffer (20 mM Tris-HCl, pH 7.6, 2.5 mM 2-ME, and 0.1 M NaCl) with or without 10^{-4} M GA_4. After incubation, 20 μL of TALON metal affinity resin was added. After further incubation at 30°C for 15 min, the resin was washed five times with washing buffer (20 mM Tris-HCl, pH 7.5, 500 mM NaCl, and 0.5% Tween 20). The washing buffer also contained 10^{-4} M GA_4 where appropriate. After washing, 10 μL of 2× SDS sample buffer were added, the mixture was heat-denatured, and the sample was loaded on a 7.5% SDS-PAGE gel, and proteins were visualized by Coomassie Brilliant Blue staining. As negative controls, samples without GST-SLR1 or Trx·His-GID1 were prepared.

Coimmunoprecipitation

Transgenic rice calli overexpressing GFP-GID1 were treated with 10^{-5} M GA_4 in 0.1% ethanol and 0.2% Tween 20 or the same solvent as a control for 5 min. The callus was harvested and ground in liquid nitrogen, and the proteins were extracted by adding 500 μL of buffer F (20 mM Tris-HCl, pH 8.0, 150 mM NaCl, 1 mM EDTA, 0.5% Tween 20, and 1× Complete tablet [Roche]). The extracts were then centrifuged at 16,000*g* for 30 min at 4°C. For each pull-down assay, 20 μL of anti-GFP antibodies raised in rabbit were added to 500 μL of the extract and rotated for 2 h at 4°C followed by the addition of 30 μL of equilibrated protein A agarose and further rotated for 1 h. The protein A agarose was washed five times with buffer G (20 mM Tris-HCl, pH 8.0, 500 mM NaCl, 1 mM EDTA, 0.5% Tween 20, and 1× Complete tablet [Roche]), and 2× SDS sample buffer was added and loaded on a 7.5% SDS-PAGE gel. The protein on the gel was transferred to the membrane and analyzed by immunoblot analysis using mouse anti-GFP antibodies or rabbit anti-SLR1 antibody. During all procedures, 10^{-4} M GA_4 was added to the assay mixture for GA_4-treated calli and was not added to the protein samples from calli not treated with GA_4. Coomassie Brilliant Blue staining was used to confirm equal loading.

Infiltration of *Nicotiana benthamiana* Leaf Epidermal Cells

N. benthamiana plants were grown under continuous light for ~1 month at 26°C. *A. tumefaciens* strain GV3101-pM90 containing an appropriate construct was grown at 30°C for 2 d in LB medium containing 50 μg/mL of kanamycin and 50 μg/mL of rifampicin. One milliliter of cultured cells was transferred to 10 mL of LB medium containing 15 μM acetosyringone, 50 μg/mL of kanamycin, and 50 μg/mL of rifampicin and further cultured at 30°C to the early stationary phase. Bacterial cells were harvested by centrifugation and suspended in 10 mM $MgCl_2$ and 150 μM acetosyringone in 10 mM MES buffer, pH 5.6, and left for 2 h at room temperature. The bacterial suspension was infiltrated into the abaxial air spaces of a leaf using a 1-mL syringe. Plants were kept for 2 d after infiltration in continuous light conditions at 26°C. EYFP and DAPI signals in leaf epidermal cells were observed using fluorescence microscopy (Olympus BX51) with U-MYFPHQ and U-MWU2 filter units, respectively.

Gel Filtration Analysis

Purified Trx·His-GID1 and Trx·His-SLR1 derivatives were mixed in a 1:1 ratio (mole/mole) estimated by each absorbance at 280 nm and incubated at 4°C for 30 min with or without 10^{-4} M GA_3 in buffer F (20 mM Tris-HCl, pH 7.5, 150 mM NaCl, and 2 mM 2-ME). One hundred microliters of the reaction mixture (50 to 100 μg of total protein) was applied to a Superdex 200 10/300 GL column (GE Healthcare) equilibrated with buffer F and eluted with the same buffer ($\pm 10^{-4}$ M GA_3) at a flow rate of 0.4 mL per minute at 4°C. Fractions (0.5 mL) were collected, and each peak fraction was analyzed by SDS-PAGE. The column was calibrated using low molecular weight markers (GE Healthcare): 25 kD chymotrypsinogen A, 43 kD ovalbumin, 67 kD albumin, and 134 kD albumin dimer. The MWs of Trx·His-GID1 and Trx·His-SLR1 derivatives were estimated from the standard curve plotted from the elution volumes of these standard proteins.

Accession Numbers

GenBank/EMBL accession numbers and Arabidopsis Genome Initiative locus identifiers for the genes mentioned in this article are as follows: *GID1* (AB211399), *SLR1* (AB262980), *GID1a* (At3g05120), *GID1b* (At3g63010), and *GID1c* (At5g27320).

Supplemental Data

The following materials are available in the online version of this article.

Supplemental Figure 1. GID1 Interacts with SLR1 in a GA_4-Dependent Manner.

Supplemental Figure 2. Recombinant GFP-GID1 Interacts with GST-SLR1 in a GA_4-Dependent Manner in Vitro.

Supplemental Figure 3. Comparison of Amino Acid Sequences of Rice and *Arabidopsis*.

Supplemental Figure 4. Loading Control for the GA Binding Experiment Using Mutagenized GID1 Proteins with Conserved Amino Acids Replaced with Ala.

Supplemental Table 1. Primers Used in This Study.

ACKNOWLEDGMENTS

We thank Yasufumi Daimon and Takashi Araki of Kyoto University for providing the vector and technical advice about BiFC as well as Hirofumi Yoshioka and Yoshihiro Kobae of Nagoya University for technical advice about fluorescent microscopy and infiltration of *N. benthamiana* leaf epidermal cells. We thank Ryoko Kigaku, Mayuko Kawamura, and Hitomi Kihara for expert technical assistance. This work was supported in part by the Ministry of Education, Culture, Sports, Science, and Technology of Japan (Grant-in-Aid for Scientific Research [M.M., I.Y., M.N, M.U.-T., and H.K.] and Target Proteins Research Program [M.M.]) and by a grant from the Ministry of Agriculture, Forestry, and Fisheries of Japan (Green Technology Project IP-1003; M.A. and M.M.).

Received April 26, 2007; revised June 28, 2007; accepted June 30, 2007; published July 20, 2007.

REFERENCES

Abe, M., Kobayashi, Y., Yamamoto, S., Daimon, Y., Yamaguchi, A., Ikeda, Y., Ichinoki, H., Notaguchi, M., Goto, K., and Araki, T. (2005). FD, a bZIP protein mediating signals from the floral pathway integrator FT at the shoot apex. Science **309:** 1052–1056.

Chandler, P.M., Marion-Poll, A., Ellis, M., and Gubler, F. (2002). Mutants at the *Slender1* locus of barley cv Himalaya: Molecular and physiological characterization. Plant Physiol. **129:** 181–190.

Cuff, J.A., Clamp, M.E., Siddiqui, A.S., Finlay, M., and Barton, G.J. (1998). Jpred: A consensus secondary structure prediction server. Bioinformatics **14:** 892–893.

Davies, P.J. (1995). Plant Hormones. (Dordrecht, The Netherlands: Kluwer Academic Publishers).

De Simone, G., Galdiero, S., Manco, G., Lang, D., Rossi, M., and Pedone, C. (2000). A snapshot of a transition state analogue of a novel thermophilic esterase belonging to the subfamily of mammalian hormone-sensitive lipase. J. Mol. Biol. **303:** 761–771.

De Simone, G., Menchise, V., Manco, G., Mandrich, L., Sorrentino, N., Lang, D., Rossi, M., and Pedone, C. (2001). The crystal structure

of a hyper-thermophilic carboxylesterase from the archaeon *Archaeoglobus fulgidus*. J. Mol. Biol. **314:** 507–518.

Griffiths, J., Murase, K., Rieu, I., Zentella, R., Zhang, Z.-L., Powers, S.J., Gong, F., Phillips, A.L., Hedden, P., Sun, T.-P., and Thomas, S.G. (2006). Genetic characterization and functional analysis of the GID1 gibberellin receptors in *Arabidopsis*. Plant Cell **18:** 3399–3414.

Ikeda, A., Ueguchi-Tanaka, M., Sonoda, Y., Kitano, H., Koshioka, M., Futsuhara, Y., Matsuoka, M., and Yamaguchi, J. (2001). slender rice, a constitutive gibberellin response mutant is caused by a null mutation of the *SLR1* gene, an ortholog of the height-regulating gene *GAI*/*RGA*/*RHT*/*D8*. Plant Cell **13:** 999–1010.

Itoh, H., Sasaki, A., Ueguchi-Tanaka, M., Ishiyama, K., Kobayashi, M., Hasegawa, Y., Minami, E., Ashikari, M., and Matsuoka, M. (2005). Dissection of the phosphorylation of rice DELLA protein, SLENDER RICE1. Plant Cell Physiol. **46:** 1392–1399.

Itoh, H., Tatsumi, T., Sakamoto, T., Otomo, K., Toyomasu, T., Kitano, H., Ashikari, M., Ichihara, S., and Matsuoka, M. (2004). A rice semi-dwarf gene, *Tan-Ginbozu* (*D35*), encodes the gibberellin biosynthesis enzyme, ent-kaurene oxidase. Plant Mol. Biol. **54:** 533–547.

Itoh, H., Ueguchi-Tanaka, M., Sato, Y., Ashikari, M., and Matsuoka, M. (2002). The gibberellin signaling pathway is regulated by the appearance and disappearance of SLENDER RICE1 in nuclei. Plant Cell **14:** 57–70.

Iuchi, S., Suzuki, H., Kim, Y.-C., Iuchi, A., Kuromori, T., Ueguchi-Tanaka, M., Asami, T., Yamaguchi, I., Matsuoka, M., Kobayashi, M., and Nakajima, M. (2007). Multiple loss-of-function of *Arabidopsis* gibberellin receptor AtGID1s completely shuts down a gibberellin signal. Plant J. **50:** 958–966.

Kobayashi, M., Yamaguchi, I., Murofushi, N., Ota, Y., and Takahashi, N. (1988). Fluctuation and localization of endogenous gibberellins in rice. Agric. Biol. Chem. **52:** 1189–1194.

Luo, A., et al. (2006). *EUI1*, encoding a putative cytochrome P450 monooxygenase, regulates internode elongation by modulating gibberellin responses in rice. Plant Cell Physiol. **47:** 181–191.

McGinnis, K.M., Thomas, S.G., Soule, F.D., Strader, L.C., Zale, J.M., Sun, T.-p., and Steber, C.M. (2003). The *Arabidopsis SLEEPY1* gene encodes a putative F-box subunit of an SCF E3 ubiquitin ligase. Plant Cell **15:** 1120–1130.

Nakajima, M., et al. (2006). Identification and characterization of *Arabidopsis* gibberellin receptors. Plant J. **46:** 880–889.

Naridini, M., and Dijkstra, B.W. (1999). α/β Hydrolase fold enzymes: The family keeps growing. Curr. Opin. Struct. Biol. **9:** 732–737.

Nishijima, T., Koshioka, M., and Yamazaki, H. (1993). A highly-sensitive rice seedling bioassay for the detection of femtomole quantities of 3β-hydroxylated gibberellins. Plant Growth Regul. **13:** 241–247.

Osterlund, T. (2001). Structure-function relationships of hormone-sensitive lipase Eur. J. Biochem. (Tokyo) **268:** 1899–1907.

Peng, J., Carol, P., Richards, D.E., King, K.E., Cowling, R.J., Murphy, G.P., and Harberd, N.P. (1997). The Arabidopsis *GAI* gene defines a signaling pathway that negatively regulates gibberellin responses. Genes Dev. **11:** 3194–3205.

Peng, J., et al. (1999). 'Green revolution' genes encode mutant gibberellin response modulators. Nature **400:** 256–261.

Sakai, M., Sakamoto, T., Saito, T., Matsuoka, M., Tanaka, H., and Kobayashi, M. (2003). Expression of novel rice gibberellin 2-oxidase gene is under homeostatic regulation by biologically active gibberellins. J. Plant Res. **116:** 161–164.

Sasaki, A., Itoh, H., Gomi, K., Ueguchi-Tanaka, M., Ishiyama, K., Kobayashi, M., Jeong, D.H., An, G., Kitano, H., Ashikari, M., and Matsuoka, M. (2003). Accumulation of phosphorylated repressor for gibberellin signaling in an F-box mutant. Science **299:** 1896–1898.

Silverstone, A.L., Ciampaglio, C.N., and Sun, T.-p. (1998). The Arabidopsis *RGA* gene encodes a transcriptional regulator repressing the gibberellin signal transduction pathway. Plant Cell **10:** 155–169.

Tsunoda, Y., Sakai, N., Kikuchi, K., Katoh, S., Akagi, K., Miura-O., J., Tashiro, Y., Murata, K., Shibuya, N., and Katoh, E. (2005). Improving expression and solubility of rice proteins produced as fusion proteins in *Escherichia coli*. Protein Expr. Purif. **42:** 267–277.

Ueguchi-Tanaka, M., Ashikari, M., Nakajima, M., Itoh, H., Katoh, E., Kobayashi, M., Chow, T.-Y., Hsing, Y.-i., Kitano, H., Yamaguchi, I., and Matsuoka, M. (2005). *GIBBERELLIN INSENSITIVE DWARF1* encodes a soluble receptor for gibberellin. Nature **437:** 693–698.

Wei, Y., Contreras, J.A., Sheffield, P., Osterlund, T., Derewenda, U., Kneusel, R.E., Matern, U., Holm, C., and Derewenda, Z.S. (1999). Crystal structure of brefeldin A esterase, a bacterial homolog of the mammalian hormone-sensitive lipase. Nat. Struct. Biol. **6:** 340–345.

Willige, B.C., Ghosh, S., Nill, C., Zourelidou, M., Dohmann, E.M.N., Maier, A., and Schwechheimer, C. (2007). The DELLA domain of GA INSENSITIVE mediates the interaction with the GA INSENSITIVE DWARF1A gibberellin receptor of *Arabidopsis*. Plant Cell **19:** 1209–1220.

Yeaman, S.J. (2004). Hormone-sensitive lipase-new roles for an old enzyme. Biochem. J. **379:** 11–22.

Zhu, Y., et al. (2006). *ELONGATED UPPERMOST INTERNODE* encodes a cytochrome P450 monooxygenase that epoxidizes gibberellins in a novel deactivation reaction in rice. Plant Cell **18:** 442–456.